



Identification and quantification of phosphatidylcholines containing very-long-chain polyunsaturated fatty acid in bovine and human retina using liquid chromatography/tandem mass spectrometry

Olivier Berdeaux, Pierre Juaneda, Lucy Martine, Stéphanie Cabaret, Lionel Bretillon, Niyazi Acar

► To cite this version:

Olivier Berdeaux, Pierre Juaneda, Lucy Martine, Stéphanie Cabaret, Lionel Bretillon, et al.. Identification and quantification of phosphatidylcholines containing very-long-chain polyunsaturated fatty acid in bovine and human retina using liquid chromatography/tandem mass spectrometry. *Journal of Chromatography*, 2010, 1217 (49), pp.7738-7748. <10.1016/j.chroma.2010.10.039>. <hal-01137063>

HAL Id: hal-01137063

<https://hal.archives-ouvertes.fr/hal-01137063>

Submitted on 30 Mar 2015

HAL is a multi-disciplinary open access archive for the deposit and dissemination of scientific research documents, whether they are published or not. The documents may come from teaching and research institutions in France or abroad, or from public or private research centers.

L'archive ouverte pluridisciplinaire **HAL**, est destinée au dépôt et à la diffusion de documents scientifiques de niveau recherche, publiés ou non, émanant des établissements d'enseignement et de recherche français ou étrangers, des laboratoires publics ou privés.

Accepted Manuscript

Title: Identification and quantification of phosphatidylcholines containing very-long-chain polyunsaturated fatty acid in bovine and human retina using liquid chromatography/tandem mass spectrometry

Authors: Olivier Berdeaux, Pierre Juaneda, Lucy Martine, Stephanie Cabaret, Lionel Bretillon, Niyazi Acar

PII: S0021-9673(10)01402-0
DOI: doi:10.1016/j.chroma.2010.10.039
Reference: CHROMA 351468

To appear in: *Journal of Chromatography A*

Received date: 23-7-2010
Revised date: 9-9-2010
Accepted date: 7-10-2010

Please cite this article as: O. Berdeaux, P. Juaneda, L. Martine, S. Cabaret, L. Bretillon, N. Acar, Identification and quantification of phosphatidylcholines containing very-long-chain polyunsaturated fatty acid in bovine and human retina using liquid chromatography/tandem mass spectrometry, *Journal of Chromatography A* (2008), doi:10.1016/j.chroma.2010.10.039

This is a PDF file of an unedited manuscript that has been accepted for publication. As a service to our customers we are providing this early version of the manuscript. The manuscript will undergo copyediting, typesetting, and review of the resulting proof before it is published in its final form. Please note that during the production process errors may be discovered which could affect the content, and all legal disclaimers that apply to the journal pertain.



1 **Identification and quantification of phosphatidylcholines containing very-long-chain**
2 **polyunsaturated fatty acid in bovine and human retina using liquid chromatography/tandem**
3 **mass spectrometry.**

4 Olivier Berdeaux¹, Pierre Juaneda², Lucy Martine², Stephanie Cabaret¹, Lionel Bretillon² and Niyazi Acar²

5

6 ¹ Lipid-Aroma Platform, Centre des Sciences du Goût et de l'Alimentation, UMR6265 CNRS, UMR1324 INRA,
7 Université de Bourgogne, Agrosup Dijon, F-21000 Dijon.

8

9 ² Eye and Nutrition Research Group, Centre des Sciences du Goût et de l'Alimentation, UMR6265 CNRS,
10 UMR1324 INRA, Université de Bourgogne, Agrosup Dijon, F-21000 Dijon.

11

12 **Address for Correspondence:**

13 Olivier Berdeaux, PhD

14 Centre des Sciences du Goût et de l'Alimentation,

15 Plate-Forme "Lipides-Arômes",

16 17, rue Sully, BP86510

17 21065 Dijon Cedex

18 France

19 Fax +33-(0)3.80.69.32.23

20 Tel. +33-(0)3.80.69.35.40

21 E-mail: berdeaux@dijon.inra.fr

22

22 Abstract

23 The retina is one of the vertebrate tissues with the highest content in polyunsaturated fatty acids
24 (PUFA). A large proportion of retinal phospholipids, especially those found in photoreceptor
25 membranes, are dipolyunsaturated molecular species. Among them, dipolyunsaturated
26 phosphatidylcholine (PC) molecular species are known to contain very-long-chain polyunsaturated
27 fatty acids (VLC-PUFA) from the n-3 and n-6 series having 24-36 carbon atoms (C24-C36) and four to
28 six double bonds. Recent interest in the role played by VLC-PUFA arose from the findings that a
29 protein called Elongation of very-long-chain fatty acids 4 (ELOVL4) is involved in their biosynthesis
30 and that mutations in the *ELOVL4* gene are associated with Stargardt-like macular dystrophy (STD3),
31 a dominantly inherited juvenile macular degeneration leading to vision loss. The aim of the present
32 study was to develop an HPLC-ESI-MS/MS method for the structural characterisation and the
33 quantification of dipolyunsaturated PC molecular species containing VLC-PUFA and validate this
34 methodology on retinas from bovines and human donors. Successful separation of
35 phosphatidylethanolamine (PE), phosphatidylinositol (PI), phosphatidylserine (PS), PC, lyso-
36 phosphatidylcholine (LPC) and sphingomyelin (SM) was achieved using a silica gel column and a
37 gradient of hexane/isopropanol/water containing ammonium formate as a mobile phase. A complete
38 structural characterisation of intact phosphatidylcholine species was obtained by collision-induced
39 dissociation (CID) in the negative mode. Fatty acid composition and distribution can be clearly
40 assigned based on the intensity of *sn*-2/*sn*-1 fragment ions. The PC species were characterised on
41 bovine retina, 28 of which were dipolyunsaturated PC species containing one VLC-PUFA (C24-C36)
42 with three to six double bonds. VLC-PUFA was always in the *sn*-1 position whilst PUFA at the *sn*-2
43 position was exclusively docosahexaenoic acid (DHA, C22:6n-3). Most of these VLC-PUFA-containing
44 dipolyunsaturated PCs were detected and quantified in human retinas. The quantitative analysis of the
45 different PC molecular species was performed in the positive mode using precursor ion scanning of
46 *m/z* 184 and 14:0/14:0-PC and 24:0/24:0-PC as internal standards. The relationship between the MS
47 peak intensities of different PC species and their carbon chain length was included for calibration. The
48 main compounds represented were those having VLC-PUFA with 32 carbon atoms (C32:3, C32:4,
49 C32:5 and C32:6) and 34 carbon atoms (C34:3, C34:4, C34:5 and C34:6). Dipolyunsaturated PCs
50 with 36:5 and 36:6 were detected but in smaller quantities. In conclusion, this new HPLC-ESI-MS/MS
51 method is sensitive and specific enough to structurally characterise and quantify all molecular PC
52 species, including those esterified with VLC-PUFA. This technique is valuable for a precise
53 characterisation of PC molecular species containing VLC-PUFA in retina and may be useful for a
54 better understanding of the pathogenesis of STD3.

55

56 Keywords:

57 Phosphatidylcholines, Quantitative analysis, LC-ESI-MS/MS, Very-long-chain polyunsaturated fatty
58 acids, Retina.

59

60 1. Introduction

61 The retina is one of the vertebrate tissues with the highest content of polyunsaturated fatty acids
62 (PUFA). A large proportion of the retinal glycerophospholipids, especially those of photoreceptor
63 membranes, consist of dipolyunsaturated molecular species. Studies have reported that
64 dipolyunsaturated phosphatidylcholine (PC) molecular species present in both rod- and cone-
65 dominant retinas contain 22:6n-3 as one of the acyl chains, the other one being very-long-chain (C24–
66 C36) polyunsaturated fatty acids (four, five or six double bonds) [1-3]. The majority of these PC
67 species containing VLC-PUFA (VLC-PC) are localised in photoreceptor outer segments where the
68 phototransduction reactions take place [4]. In bovine photoreceptor outer segments, VLC-PC species
69 are significant components of lipid membranes since the C28-C36 VLC-PUFA represent 10 mol % of
70 total fatty acids in PCs [1].

71 Recently, at least three different mutations in a gene called *elongation of very long chain fatty acids 4*
72 (*ELOVL4*) have been identified in patients with Stargardt-like macular dystrophy type 3 (STD3), a
73 dominantly inherited form of juvenile macular degeneration leading to vision loss [5-8] Based on
74 sequence homology with ELOVL1, 2, 3, and 5 proteins, which are implicated in the elongation of
75 saturated, monounsaturated, or polyunsaturated fatty acids (PUFA) from 18 to 26 carbons, the
76 ELOVL4 protein was predicted to have similar functions [5,8-11]. These findings suggested that retinal
77 health depends on the presence of C28-C36 PUFA in addition to that of docosahexaenoic acid (DHA,
78 C22:6n-3) [12].

79 Concurrently with these biochemical and molecular studies, a transgenic mouse model of STD3
80 carrying the human pathogenic 5-bp deletion in the mouse *ELOVL4* gene was developed [13]. The
81 animals displayed a retinal phenotype resembling that of human STD3, including an early selective
82 deficiency in retinal C28–C36 acyl PCs, followed by a reduced electroretinographic response, an
83 increased accumulation of toxic *N*-retinylidene-*N*-retinylethanolamine (A2E) and a degeneration of
84 photoreceptor cells in the central retina. According to these findings, the proposed pathogenesis of
85 human STD3 is based on the alteration of rod outer segments (ROS, corresponding to the distal part
86 of retinal photoreceptor cells) composition in VLC-PUFA affecting phototransduction and leading to the
87 accumulation of toxic A2E and further to photoreceptor death [14].

88 In order to confirm this hypothesis, dipolyunsaturated PC molecular species containing VLC-PUFA in
89 retina must be precisely characterised to improve our understanding of the pathogenesis of STD3.
90 Several current approaches were used for the characterisation and quantification of VLC-PUFA or
91 VLC-PC in biological samples [1,2,4,15,16], but most of these conventional approaches are time-
92 consuming, requiring successive extraction, chromatographic steps (HPLC, TLC) and often a
93 derivatisation step before gas chromatography (GC) or gas chromatography-mass spectrometry (GC-
94 MS) analyses. Electrospray ionisation-mass spectrometry (ESI-MS) has been described as a soft
95 ionisation technology [17]. It is the most sophisticated and easiest technique for assessing the
96 phospholipid content of a biological sample because of its high sensitivity and unmatched specificity. It
97 directly analyses phospholipids as intact molecules and preserves the information based on the
98 relative position of acyl radicals on the glycerol backbone. Using standard equipment, ESI-MS has
99 been widely used for characterisation [17-23] and quantification of phospholipids [24-38]. Different
100 approaches have been adopted for the analysis of molecular species of phospholipids using ESI-MS

101 [39,40]. In some of these, crude lipid extracts were infused to the MS instrument and either direct MS
102 scans or specific precursor ion or neutral loss scans were utilised to determine the different lipid
103 species [29,34,36,39,41]. Other commonly used methods employed liquid chromatography with on-
104 line mass spectrometric detection (HPLC-ESI-MS) [18,22,23,25-28,31,33,35,42-44]. The combination
105 of high-performance liquid chromatography (HPLC) and ESI-MS reduces the ionisation suppression
106 effect of low abundance PL species compared to indirect ESI-MS alone [24,43,45]. Moreover, HPLC-
107 ESI-MS offers the advantage of a low spectral background signal [46]. However, the quantitative
108 analysis of PL is not as easy since MS signals of PL are influenced by different effects related to acyl
109 chain length, the degree of acyl chain unsaturation and concentration [28,34,36].

110 In this study, we propose to develop a normal-HPLC-ESI-MS/MS method using a triple quadrupole
111 mass spectrometer for precise characterisation and quantification of major PC species (including VLC-
112 PC and glyceroplasmethylcholine plasmalogen (PLsC) species) in total lipid extracts from bovine and
113 human retinas. During the quantification step, particular attention was paid to the influence of different
114 parameters related to PC acyl chain length and the degree of acyl chain unsaturation of the
115 concentration on the spectrometer response according to previous studies [27,34,36].

116 **2. Material and methods**

117 **2.2. Lipids and other materials**

118 All chemical reagents were purchased from Sigma-Aldrich (St Quentin Fallavier, France), chloroform
119 and methanol from SDS (Peypin, France). HPLC-grade N-hexane, chloroform and isopropanol, LC-
120 MS-grade methanol and water were all from Fisher Scientific (Illkirch, France). Commercially available
121 phospholipids were obtained from Avanti Polar Lipids Inc. (Alabaster, AL, USA): dimyristoyl-*sn*-
122 glycerol-3-phosphatidylcholine (PC 14:0/14:0), 1,2-dipalmitoyl-*sn*-glycerol-3-phosphocholine (PC
123 16:0/16:0), 1-palmitoyl-2-oleoyl-*sn*-glycerol-3-phosphocholine (PC 16:0/18:1), 1,2-distearoyl-*sn*-
124 glycerol-3-phosphocholine (PC 18:0/18:0), 1-stearoyl-2-arachidonoyl-*sn*-glycerol-3-phosphocholine (PC
125 18:0/20:4), 1-stearoyl-2-arachidonoyl-*sn*-glycerol-3-phosphocholine (PC 18:0/20:4), 1-stearoyl-2-
126 docosahexaenoyl-*sn*-glycerol-3-phosphocholine (PC 18:0/22:6), 1,2-diarachidoyl-*sn*-glycerol-3-
127 phosphocholine (PC 20:0/20:0), 1,2-didocosahexaenoyl-*sn*-glycerol-3-phosphocholine (PC 22:6/22:6),
128 1,2-dilignoceroyl-*sn*-glycerol-3-phosphocholine (PC 24:0/24:0), 1-(1Z-octadecenyl)-2-oleoyl-*sn*-glycerol-
129 3-phosphocholine (PLsC p180/18:1, where p refers to the ether-linked alcohol), 1-(1Z-octadecenyl)-2-
130 docosahexaenoyl-*sn*-glycerol-3-phosphocholine (PLsC p180/22:6) and mixture PC molecular species
131 of brain porcine.

132 **2.3. Lipid extraction**

133 Eyeballs were collected from a calf as well as from nine human donors according to a previously
134 published procedure [47]. Samples from human cadavers were collected in accordance with the
135 guidelines of the Declaration of Helsinki. Human eyeballs were obtained from 9 donors (bodies
136 donated to science, five women and four men; mean age, 84.3 ± 8.5 years; range, 72–97 years)
137 within 16 h (median time, mean time 15 ± 7 h) after death. The bodies were refrigerated at 4°C in the
138 first hours after death (less than 24 h). Eyeballs were enucleated at the anatomy laboratory of the

139 Saint-Etienne School of Medicine (France). Enucleated eyeballs were immersed in balanced salt
140 solution (BSS, Alcon, Rueil Malmaison, France) at 4°C. Within 30 min after enucleation, a circular
141 section at the pars plana was taken with an 18-mm-diameter trephine and the corneoscleral disc
142 removed for other studies. The posterior pole was placed on a back-lit table and the retina was
143 observed under an operating microscope to select the tissue included in this study. Eyes with large
144 drusen or severe pigment epithelial alterations, severe macular atrophy, macular hemorrhage, or any
145 grossly visible chorioretinal pathologic abnormality were excluded. The vitreous body was carefully
146 removed. The entire neural retina was carefully separated with forceps. Samples were stored at -80°C
147 under argon atmosphere. Total lipids were extracted from retinas according to the method described
148 by Folch *et al.* (1957) [48]. The phosphorus content of the total phospholipid extract was determined
149 according to the method developed by Bartlett and Lewis [49]. The total phospholipids were dried
150 under a stream of nitrogen, after which internal standards PC 14:0/14:0 (final concentration, 0.4 ng/μL)
151 and PC 24:0/24:0 (final concentration, 0.64 ng/μL) were added at about 30% of the major PC
152 molecular species. The samples were then diluted to the appropriate concentration of 12.5 ng/μL in
153 chloroform/methanol (1:1, v/v) for analysis and stored at -80°C under argon atmosphere.

154 **2.4. LC-ESI-MS using triple-quadrupole mass spectrometer**

155 The total phospholipids were analysed by liquid chromatography coupled to a mass spectrometer
156 equipped with an ESI source. HPLC was performed using a JASCO PU 2089 Plus LC pump equipped
157 with a JASCO AS 2057 Plus auto-sampler from JASCO Analytical Instruments (Bouguenais, France).
158 The injection volume was 5 μL. The separation was performed using a Hypersil Silica Column (150
159 mm × 2.1 mm, i.d. × 3 μm) from ThermoFinnigan (San Jose, CA, USA). The mobile phase consisted
160 of (A) hexane/2-propanol/chloroform/water (44/43.5/10.5/2, v/v/v/v) containing 12.5 mM of ammonium
161 formate and (B) hexane/2-propanol/chloroform/water (34/49/10.5/6.5, v/v/v/v) containing 12.5 mM of
162 ammonium formate. The solvent-gradient system comprised as follows: 0 min A/B (%) 100/0, 10.5–24
163 min A/B (%) 22/78, 26.5–45 min A/B (%) 0/100% and 46–60 min A/B (%) 100/0. The flow rate was 300
164 μL.min⁻¹ and the column was maintained at 30°C. The flow from LC was split using an analytical fixed
165 flow splitter (split ratio = 1:1, post-column) from Analytical Scientific Instruments (El Sobrante, CA,
166 USA). Mass spectrometry was performed using a ThermoFinnigan TSQ Quantum triple quadrupole
167 mass spectrometer equipped with a standard electrospray ionisation source outfitted with a 100-μm
168 i.d. H-ESI needle. The source spray head was oriented at a 90° angle orthogonal to the ion-transfer
169 tube. Nitrogen was used for both the sheath and the auxiliary gases. The MS signals of PC species
170 were first optimised by continuous infusion of the standards dissolved in the mobile phase using ESI in
171 negative and positive modes. The electrospray ionisation spray voltages were 3 kV and -4.5 kV in
172 negative and positive ion modes, respectively, vaporiser temperature was 150°C, sheath gas N₂
173 pressure 45 (arbitrary units), auxiliary gas pressure 45 (arbitrary units), ion sweep gas pressure 5, ion
174 transfer capillary temperature 300°C, skimmer offset 5 V and multiplier gain 300,000.

175 When operated under full scan conditions in the negative and positive ion modes, data were collected
176 in the range of *m/z* 400–1100 with a scan time of 0.5 s. For PC characterisation in the negative mode,
177 ESI-MS/MS was used with argon as the collision gas at 1.5 mTor, and the collision energy was set to

178 15 eV; in the positive mode, the collision gas pressure was 0.8 mTor and the collision energy ranged
179 from 30 to 45eV. PC species were manually identified with the parent mass information and their
180 characteristic fragment ions in the CID spectrum using lists of PL species prepared in our laboratory.

181 For PC quantification in ESI/MS/MS, precursor scanning at m/z 184 was used. Optimum conditions for
182 collision-induced dissociation (CID) were selected. For all calculations, the ratio of peak area of each
183 PC species to the peak area of the internal standards (PC 14:0/14:0 and PC 24:0/24:0) was used.
184 Corrections are applied to the data for isotopic overlap. The data were processed using the Xcalibur
185 software (ThermoFinnigan).

186 **2.5. Preparation of fatty acid methyl esters**

187 The fatty acid methyl esters (FAMES) were prepared using the boron trifluoride (BF_3) reagent as the
188 catalyst according to Morrison and Smith [50]. Briefly, lipids (up to 20 mg) were transferred to a
189 centrifuge tube with a PTFE-lined screw cap and evaporated under a stream of nitrogen; 0.3 mL of
190 toluene and 0.7 mL of boron trifluoride reagent (BF_3 /methanol, 7%) were added under nitrogen and
191 the tube was closed with the screw cap. The tube was then heated to 95°C for 2 h and then cooled to
192 room temperature. FAMES were extracted by adding 5 mL of saturated solution of NaHCO_3 and 3×2
193 mL of hexane. The mixture was centrifuged (3000 rpm) for 3 min to break the emulsion formed. After
194 drying the organic phase over sulfate sodium (Na_2SO_4), the solvent was removed under a stream of
195 nitrogen and FAMES were dissolved in hexane for GC analysis.

196 **2.6. Gas-chromatography analysis**

197 FAMES (0.5 mg/mL in hexane) were analysed on a Hewlett Packard Model 4890 gas-chromatograph
198 (Palo Alto, CA, USA) using a CP-Sil 88 (100 m × 0.25 mm I.D. capillary column, 0.2 μm film, Varian,
199 Courtaboeuf, France). The instrument was equipped with a split/splitless injection (splitless for 0.5
200 min). The linear velocity of hydrogen was 37.0 cm/s at 60°C. The temperature was held at 60°C for 5
201 min, raised to 165° at 15°C/min and held for 1 min and then to 225°C at 2°/min and finally held at
202 225°C for 17 min according to the procedure described in the literature [51]. The injection port was
203 held at 250°C and a flame ionisation detector (FID) was used at 250°C.

204 **2.7. Preparation of 4,4-dimethyloxazoline derivatives**

205 FAME (up to 2 mg) were converted to the 4,4-dimethyloxazoline (DMOX) derivatives by treatment with
206 250 μL of 2-amino-2-methyl-1-propanol in a test tube at 170°C overnight in a nitrogen atmosphere
207 [52]. The reaction mixture was cooled and dissolved in 3 mL of dichloromethane and further washed
208 twice with 5 mL of water. After drying the organic phase over Na_2SO_4 , the solvent was removed under
209 a stream of N_2 and the sample was dissolved in hexane for GC-MS analysis.

210 **2.8. Gas-chromatography mass-spectrometry**

211 GC-MS analyses of DMOX derivatives were carried out on an Agilent 6890 series II gas
212 chromatograph attached to an Agilent model 5973N selective quadrupole mass detector (Palo Alto,
213 CA, USA) operating in the electronic ionisation mode under an ionisation voltage of 70 eV at 230°C.
214 Agilent ChemStation software was used for data acquisition and processing. The injector (splitless

215 mode) and the interface temperature were maintained at 250°C, whereas helium was used as the
216 carrier gas under constant flow at 1 mL/min. Spectral data were acquired over a mass range of 50–
217 600 amu. GC separation was performed on a BPX-70 (60 m × 0.25 mm I.D. capillary column, 0.25 µm
218 film; SGE, Melbourne, Australia). The temperature was held at 60°C for 1 min, raised to 240 at
219 20°C/min and held at 240°C for 90 min.

220 **3. Results and discussion:**

221 The objective of the present study was to develop a sensitive and specific method for the
222 characterisation and quantification of PC species and in particular VLC-PC species in human retina
223 using LC-ESI-MS/MS. Given the greater availability of bovine retinas compared to human retinas, the
224 former were used by means of characterisation of VLC-PC. Bovine retina is also known to contain
225 VLC-PUFA (C24–C36), specifically concentrated in PC [2].

226 **3.1. Separation of phospholipid classes**

227 We chose to separate the phospholipid species using LC prior to the ESI-MS/MS analysis in order to
228 enhance the detection of the minor isobaric species in the mixture. Additionally, a suitable
229 chromatographic separation may reduce any ESI suppression of non-isobaric and co-eluting species.
230 Then we developed a normal-phase HPLC separation of phospholipid (PL) classes in order to
231 separate and study the collision-induced dissociation of these PC molecular species containing VLC-
232 PUFA using a triple-quadrupole instrument.

233 Phospholipid species are zwitterionic molecules. Therefore either positive- or negative-ion mass
234 spectra of these phospholipid classes were accessible through ESI-MS analysis. However, negative-
235 ion ESI mass spectra of phosphatidylethanolamine (PE), lyso-phosphatidylethanolamine (LPE),
236 phosphatidylinositol (PI) and phosphatidylserine (PS) species only contain the $[M-H]^-$ ion and were far
237 more sensitive than positive-ion spectra [20]. In contrast, PC, lyso-phosphatidylcholine (LPC) and
238 sphingomyelin (SM) species were more efficiently analysed in the positive-ion mode by generating
239 protonated $[M+H]^+$ ions but might also produce sodiated adduct $[M+Na]^+$ ions. Only during the
240 development of LC separation of total phospholipids was the mass spectrometer operated under full
241 scan conditions in the negative ion mode for detection of PE, PI, PS and LPE and under full scan
242 conditions in the positive ion mode for quantification of PC, LPC and SM species. A mobile phase
243 consisting of hexane/isopropanol/chloroform/water for HPLC separation of PL classes on silica
244 columns has been reported to give good separation for some PLs [53,54]. However, since PI and PS
245 as well as PC and SM eluted very closely, class determination was far more complicated. In our study,
246 ammonium formate was added to this mobile phase system to enhance separation, resolution and
247 selectivity. By optimising the concentration of ammonium formate in the mobile phase, the flow rate
248 and the use of a pertinent gradient, a good baseline separation of PE, PI, PS, PC, SM and LPC
249 classes in bovine and human retinas was achieved, as illustrated in **Fig. 1**. The method did not require
250 fractionation into neutral lipids and phospholipids. Total lipid extracts from retinas can be injected
251 directly into the system, with neutral lipids eluting with the solvent front. As expected,
252 plasmeylcholine (PlsC) species co-eluted with PC species. Moreover, under our HPLC conditions,
253 VLC-PC molecular species containing VLC-PUFA eluted separately just before other PC molecular

254 species, between 15.5 and 17 min. Also, it was possible to collect this fraction in order to concentrate
255 VLC-PC for further structure characterisation using GC-MS.

256 **3.2. Determination of PC species based on their specific fragmentation mechanisms**

257 Detailed structural analysis of glycerophospholipids can be performed using electrospray tandem
258 mass spectrometry (ESI-MS/MS). Collision-induced dissociation (CID) of $[M+H]^+$ or $[M-H]^-$ of
259 phospholipids results in fragment ions that are related to the polar head group and fatty acyl
260 substituent esterified to the glycerol backbone.

261 In order to characterise PC molecular species, lipid extracts from bovine retina were analysed by ESI-
262 MS/MS in the positive and negative modes. Mass spectra obtained by CID of PC molecular ions were
263 compared with those obtained from commercial standards. When operated in the single-stage MS
264 mode using ESI in the positive ionisation mode, PC molecular species produced abundant $[M+H]^+$ ions
265 as well as sodiated $[M+Na]^+$ ions [18]. The MS² fragmentation of the selected $[M+H]^+$ molecular ion of
266 PC and PlsC gave an intense fragment at m/z 184 derived from phosphocholine head $[C_5H_{13}NPO_4]^+$.
267 When operated in the single-stage MS mode in the negative mode ionisation, PC molecular species
268 produced abundant demethylated molecule $[M - CH_3]^-$ ions (base peak). Molecular ions $[M-H]^-$ were
269 not detected. Under our HPLC conditions with chloroform and ammonium formate, chloride- $[M+Cl]^-$
270 and formate- $[M+HCOO]^-$ adducts were also produced. By increasing the skimmer-off set value from 5
271 to 25 V, it was possible to reduce these two adducts. The MS² experiment of the selected $[M - CH_3]^-$
272 of PC species gave a characteristic fragmentation. As an example, for PC 16:0/18:1 (**Fig. 2A**), the
273 MS² fragmentation of the selected molecular ion $[M - CH_3]^-$ at m/z 744 showed two prominent ions
274 derived from the carboxylate anions at m/z 281 (major) and m/z 255 (minor), which correspond to the
275 C18:1 and C16:0 fatty acyl substituent, respectively. Elimination of the fatty acyl substituent C18:1 and
276 C16:0 leads to the formation of very minor fragments at m/z 462 and m/z 488, corresponding to the $[M$
277 $- CH_3 - R_2CHCOOH]^-$ and the $[M - CH_3 - R_1CHCOOH]^-$ ions respectively. Two other fragments at
278 m/z 480 and m/z 506 were also detected in slightly greater amounts than fragments at m/z 462 and
279 m/z 488. These fragments corresponded to the $[M - CH_3 - R_2CH=C=O]^-$ and the $[M - CH_3 -$
280 $R_1CH=C=O]^-$ ions, respectively, resulting from the loss of fatty acyl groups such as ketenes [19,21].
281 According to some authors, acyl chain distribution in phospholipids can be accurately determined with
282 a triple-quadrupole spectrometer. The intensity of the carboxylate anion derived from the *sn*-2 acyl
283 substituent is greater than the carboxylate anion derived from the *sn*-1 acyl substituent [18,19].
284 However, under our conditions, it was not verified with PC containing an LC-PUFA in position *sn*-2,
285 e.g. C20:4n-6 (**Fig. 2B**) or C22:6n-6 (**Fig. 2C**). Indeed when R_2CH_2COOH was an LC-PUFA, a
286 fragment was also detected at a mass 44 Da lower than the carboxylate anion $[R_2CH_2COO]^-$. This
287 fragment is generated by the loss of one CO₂ molecule from this LC-PUFA carboxylate anion. For
288 example, the MS² fragmentation of the selected molecular ion $[M-CH_3]^-$ at m/z 794 of PC 18:0/20:4
289 showed two prominent ions at m/z 283 (C18:0 carboxylate anion) and m/z 303 (C20:4 carboxylate
290 anion) and a lower fragment at m/z 259 generated by CO₂ loss by the C20:4 carboxylate anion. In the
291 case of PC 18:0/22:6, the fragment at m/z 327 was decreased by the loss of one CO₂ molecule from
292 the C22:6 carboxylate anion, while the fragment at m/z 283 was increased because it was the sum of

293 two fragments: the C18:0 carboxylate anion and the ion formed by the loss of 44 Da from the C22:6
294 carboxylate anion. Consequently, the intensity of the C18:0 carboxylate anion derived from the *sn*-1
295 acyl substituent was greater than the C22:6 carboxylate anion derived from the *sn*-2 acyl substituent.
296 In contrast, the regiospecificity of the acyl moieties in asymmetrical PC, even with a LC-PUFA in the
297 *sn*-2 position, can be confirmed from the packet of *sn*-1 acyl and *sn*-2 acyl lyso-PC product-ion peaks
298 because the *sn*-1 acyl lyso-PC ion is always more abundant than the *sn*-2 acyl lyso-PC ion (**Fig. 2A–**
299 **C**) [19]. For plasmalogen species, only the carboxylate anion corresponding to the *sn*-2 acyl
300 substituent was detected, since the *sn*-1 substituent did not easily cleave to form an anion [19,35] (**Fig**
301 **2D**). However, in the case of PlsC 18:0/22:6 (**Fig. 2E**), the MS² fragmentation of the selected
302 molecular ion $[M - CH_3]^-$ at *m/z* 802 shows the ion at *m/z* 327 corresponding to the C22:6 carboxylate
303 anion and the fragment at *m/z* 283, which is generated by CO₂ loss, as explained above. Thus, during
304 the interpretation of spectra from PC or PlsC containing C22:6n-3 in the *sn*-2 position, it is important to
305 pay attention to the fragment at *m/z* 283 generated by CO₂ loss by C22:6 carboxylate anion, because
306 it can be confused with the C18:0 carboxylate anion.

307 The PC species were characterised in bovine retina. The different PC, VLC-PC and PlsC molecular
308 species characterised in bovine retina (**Fig. 3A**) are listed in Table 1. We particularly focused on the
309 VLC-PC fraction in the retina (**Fig. 3B**). Identification by ESI-MS/MS showed that this fraction
310 contained exclusively dipolyunsaturated PC species with one VLC-PUFA always in the *sn*-1 position
311 and docosahexaenoic acid (DHA, C22:6n-3) exclusively at the *sn*-2 position. For example, as
312 illustrated in **Fig. 2F** the product ion spectra of the demethylated molecular ion $[M - CH_3]^-$ of PC
313 32:4/22:6 at *m/z* 1006 showed the two abundant ions at *m/z* 327 and *m/z* 471, corresponding to C22:6
314 and C32:4 carboxylate anions, respectively, and the ion at *m/z* 283, which is generated by CO₂ loss by
315 the C22:6 carboxylate anion. Furthermore, we observed the product ions formed by neutral loss of
316 either an FA or a ketene at *m/z* 678 ($[M - CH_3 - R_2CH-COOH]^-$), *m/z* 696 ($[M - CH_3 - R_2CH=C=O]^-$),
317 and *m/z* 552 ($[M - CH_3 - R_1CH=C=O]^-$). Among these three fragments, the fragment at *m/z* 696 was
318 the most abundant and it was therefore useful for regioisomeric assignment.

319 We characterised 69 PC molecular species, in particular 22 VLC-PC molecular species, in bovine
320 retina (**Table 1**). All these identified VLC-PC molecular species contained C22:6 in the *sn*-2 position
321 and VLC-PUFA in the *sn*-1 position according to Aveldaño [55]. These VLC-PC species contained
322 fatty acyl from 24 to 36 carbon chains long, with four, five or six double bonds. The majority of VLC-PC
323 contained C32 and C34 VLC-PUFA with four, five or six double bonds. Phospholipids from human
324 retina were also separated (**Fig. 1B**) using the same LC-ESI-MS conditions. The main PC and VLC-
325 PC were characterised and compared to those identified in bovine retina (**Fig. 4**). Thirty-six PC
326 molecular species and in particular 13 VLC-PC molecular species were detected in significant
327 amounts in human retina (**Table 2**). Similar structures of VLC-PC to those in bovine retina were
328 characterised in human retina. C22:6 still remained in the *sn*-2 position and the VLC-PUFA in the *sn*-1
329 position. Moreover, as in bovine retina, the majority of VLC-PC contained C32 and C34 VLC-PUFA
330 with four, five or six double bonds. Only traces of VLC-PC containing C30:5, C30:6, C36:5 and C36:6
331 were also detected but could not be quantified.

332 For structural identification of VLC-PUFA, LC-MS/MS did not allow localisation of the double bonds
333 along the carbon chain. According to previous studies, retinal C28-C36 fatty acids are polyunsaturated
334 and belong to the n-3 and n-6 families [2,56]. The n-6 family of C28-C36 fatty acids has four or five
335 double bonds, while the n-3 family of VLC-PUFA contain five or six double bonds. To check these in
336 our retina samples, a part of the isolated VLC-PC fraction by HPLC was converted into fatty acid
337 methyl esters (FAMES) and analysed by GC-FID). An aliquot of FAME of the isolated VLC-PC fraction
338 from bovine retina was then converted into DMOX derivative and analysed using GC-EI-MS (**Fig. 5A**).
339 Identification was established according to previous studies [52,57,58]. For example, the mass spectra
340 of the DMOX derivative of C32:4 (n-6) and C32:6 (n-3) are presented in **Fig. 6**. GC-MS mass spectra
341 of DMOX derivative of C32:6 n-3 and 32:4 n-6 gave intense molecular ions at m/z 521 and m/z 525
342 respectively, and fragmentation localised the double bonds in the carbon chain. In DMOX derivatives
343 of mono- or polyunsaturated fatty acids, a mass interval of 12 amu instead of the regular 14 amu
344 between two neighbouring homologous fragments containing n-1 and n carbon atoms of the original
345 acid moiety indicates that a double bond exists between carbons n and n+1 in the chain [58].
346 Moreover, it is important to note that a gap of 40 amu is also observed between the two fragments
347 containing n-2 and n+1 carbon atoms, located around the double bond. Thus, we have established the
348 mass spectra of the DMOX derivatives of major VLC-PUFA detected in the isolated VLC-PC fraction
349 obtained by HPLC from bovine and human retinas (**Fig. 6A and 6B**). In our samples of bovine retinas,
350 as in human retinas, C30-C34 VLC-PUFA of the n-6 family had only four double bonds, while C28-
351 C36 VLC-PUFA of the n-3 family had five or six double bonds. Moreover, as expected, C32 and C34
352 VLC-PUFA with four, five and six double bonds seem to represent the prominent VLC-PUFA in bovine
353 retinas as well as in human retinas. These results are in agreement with our LC-MS/MS data.

354 PUFA longer than C26 are suspected of having key functions in several tissues. For example, they are
355 essential components of epidermal acylceramides and then important actors in skin barrier function
356 [59,60], whereas they were shown to be involved in sperm maturation in testis [61,62]. In the retina,
357 C28-C36 VLC-PUFA appear to be associated with rhodopsin in photoreceptor outer segments [55]
358 and are suspected of being involved in phototransduction processes. This hypothesis is consistent
359 with the electroretinographic defects in the various mouse models carrying various mutations in the
360 *ELOVL4* gene [13,63-65], even if their retinas have not been fully characterised in terms of changes in
361 C28-C36 acyl PCs.

362 **3.3. Quantification of the PC species in total lipids extracted from human retina**

363 In single-stage positive-ion ESI-MS of total lipid extracts, PC molecular species often give rise to major
364 peaks corresponding to the sodiated molecular ions $[M+Na]^+$ along with the protonated ones $[M+H]^+$.
365 This phenomenon, also reported previously [17-19,36], complicates the analysis of PCs in biological
366 samples. Addition of ammonium formate in the LC solvent considerably reduced the formation of
367 sodiated adducts $[M+Na]^+$ (<5%) but did not eliminate them completely [31]. Alternatively, some
368 authors included sodium or lithium salts to suppress formation of protonated ions [19,66]. However,
369 we were not able to avoid protonated ions by post-column inclusion of lithium or sodium salts, directly
370 in the source. In the MS² mode, PC species showed an intense fragment at m/z 184 due to their

371 choline head group. This fragment was used for precursor ion scanning, whereby the $[M+H]^+$ ions of
372 PCs are specifically detected [29,30,36]. Precursor ion scanning for m/z 184 selectively detects only
373 $[M+H]^+$ ions for choline-containing phospholipids, since PC molecules cationised by sodium or
374 potassium exclusively lose their polar choline phosphate head group as a 183-Da neutral fragment
375 instead of forming the fragment at m/z 184 [34]. To optimise the formation of this precursor, we
376 investigated the influence of the fatty acid chain length on the intensity and optimal collision cell offset
377 for the generation of the m/z 184 fragment for PC 14:0/14:0 (PC 28:0), PC 16:0/16:0 (PC 32:0), PC
378 18:0/18:0 (PC 36:0), PC 20:0/20:0 (PC 40:0), PC 23:0/23:0 (PC 46:0), PC 24:0/24:0 (PC 48:0), PC
379 16:0/18:1 (PC 34:1), PC 18:0/18:2 (PC 36:2), PC 18:0/20:4 (PC 38:4), PC 18:0/22:6 (PC 40:6), PC
380 22:6/22:6 (PC 44:12) and PlsC 18:0/22:6 (PlsC 40:6). Collision cell offset plots were established
381 correlating the fragment ion intensity at m/z 184 with the voltage off in the collision cell. Moreover,
382 collision cell offset plots were also established for the more intense VLC-PUFA, PC 32:4/22:6 (PC
383 54:10, m/z 1022) and PC 34:4/22:6 (PC 56:10, m/z 1050) using the isolated and concentrated HPLC
384 fraction containing VLC-PC. As a result, the optimal collision offset increases with increasing chain
385 length, varying from about -30 to -50 V for the precursor ions investigated. As a compromise, -36 V
386 was selected as collision cell offset.

387 Determination of phospholipid molecule species level requires the addition of internal standards
388 because the ionisation efficiency between different phospholipid classes of ESI-MS may differ
389 significantly with respect to experimental conditions. PC 14:0/14:0 (m/z 678) and PC 24:0/24:0 (m/z
390 958) were selected as internal standards in the analyses of PC, PlsC and VLC-PC since these
391 molecular species do not occur naturally in biological samples studied in this work. However,
392 precautions were taken in this quantitative study because different molecular species are not detected
393 with equal efficiency. Previous studies indicated that the total phospholipid concentration affect the
394 quantification of PC species by ESI-MS/MS [29]. Therefore, we investigated the influence of these
395 different parameters on the instrument response. First, to establish the range of linear response of our
396 ESI-MS/MS instrument, an equimolar mixture was prepared with standards of PC 14:0/14:0, PC
397 16:0/16:0, PC 16:0/18:1, PC 18:0/18:0, PC 18:0/18:2, PC 18:0/20:4, PC 18:0/22:6, PlsC 18:0/22:6, PC
398 20:0/20:0, PC 22:6/22:6, PC 23:0/23:0 and PC 24:0/24:0, diluted from 5 $\mu\text{g}/\mu\text{L}$ to 5 $\text{ng}/\mu\text{L}$ per species
399 (from 60 $\mu\text{g}/\mu\text{L}$ to 60 $\text{ng}/\mu\text{L}$ of total PC) in chloroform/methanol (1:1) and then injected to LC-ESI-MS.
400 The PC mixture had a linear response of ion count versus concentration from 5 μg to 2 $\text{ng}/\mu\text{L}$ (from 60
401 $\mu\text{g}/\mu\text{L}$ to 24 $\text{ng}/\mu\text{L}$ of total PC) (**Fig. 7**). Beyond this concentration, the response was nonlinear and
402 began to plateau.

403 Furthermore, the acyl chain length and chain unsaturation have a significant effect on the instrument
404 response [28,34,36,67]. We established a calibration curve between the intensity of the observed
405 quasi-molecular ion species and the length and degree of unsaturation of the carbon chains.
406 Response curves were prepared with increased concentrations of PC 16:0/16:0, PC 16:0/18:1, PC
407 18:0/18:2, PC 18:0/18:0, PC 18:0/20:4, PC 18:0/22:6, PlsC 18:0/22:6, PC 20:0/20:0, PC 22:6/22:6 and
408 PC 23:0/23:0 (range, 2.5 $\mu\text{g}/\mu\text{L}$ to 2.5 $\text{ng}/\mu\text{L}$) and fixed concentrations of PC14/14:0 (0.4 $\text{ng}/\mu\text{L}$) and
409 PC 24:0/24:0 (0.64 $\text{ng}/\mu\text{L}$) as internal standards. Linear calibration curves were obtained for PC
410 species from 2.5 $\mu\text{g}/\mu\text{L}$ to 2.5 $\text{ng}/\mu\text{L}$. Our results confirmed that the instrument response for PC

411 species decreases when the phospholipid acyl chain length is increased [28,34,36]. According to
412 Koivusalo et al. [36], the responses remain a linear function of the acyl chain length, even at the
413 highest concentrations. Lastly, under our conditions, the effect of acyl chain unsaturation seems to be
414 weak. Previous studies showed that the effect of acyl chain unsaturation was less significant when the
415 injection amount of lipid molecules is minimised [27,36]. To overcome this problem, experiments were
416 conducted with the least amount of required material.

417 After having determined the effect of structural factors and lipid concentration on the instrument, we
418 used this information to quantify the molecular species of PC and PlsC in human retina. In order to
419 check the applicability of the method in a biological sample, samples of human retina (12.5 ng/μL) or
420 blank (chloroform/methanol) were spiked with the increment level of an equimolar mixture of saturated
421 PC 14:0/14:0, PC 18:0/18:0, PC 20:0/20:0, PC 23:0/23:0 and PC 24:0/24:0 (0.25, 0.5 or 1 ng/μL per
422 species), and then analysed. An example of representative spectrum is shown in **Fig. 8**. These
423 allowed us to correct for acyl chain length dependency of the instrument response. Consequently, a
424 calibration function was then calculated and used to correct the experimental ion abundance in order
425 to obtain the true molar abundance. With VLC-PUFA (from PC 52:9 and PC 58:10), no standards were
426 available to calculate the calibration curve. Therefore, this curve was extrapolated from the different
427 results obtained above as a function of the phospholipid acyl chain length and the degree of acyl chain
428 unsaturation.

429 The calibration method developed was then applied to quantify PC and VLC-PC molecular species
430 extracted from retina samples obtained from nine human donors. The phosphorus content of total lipid
431 extracts was determined using the Bartlett and Lewis method [49] in order to standardise the
432 concentration of all lipid extracts at 12.5 ng/μL. A constant amount of both PC 14:0/14:0 (0.4 ng/μL)
433 and PC 24:0/24:0 (0.64 ng/μL) were therefore added to an aliquot of the lipid extract (12.5 ng/μL) for
434 the quantification. PC 24:0/24:0 was added with a known amount in order to estimate the accuracy of
435 the MS method for every sample. The identified and quantified 36 PC species in human retinas are
436 listed in **Table 2**. In most of these, 13 VLC-PUFA-containing dipolyunsaturated PC were detected and
437 quantified. The main VLC-PC (PC containing VLC-PUFA) detected and quantified in human neural
438 retinas were those having VLC-PUFA of 32 carbon atoms (C32:3, C32:4, C32:5 and C32:6) and 34
439 carbon atoms (C34:3, C34:4, C34:5 and C34:6). Dipolyunsaturated PC with 30:5, 30:6, 36:5 and 36:6
440 were detected but in smaller quantities.

441 **4. Conclusion**

442 In summary, qualitative and quantitative analysis of VLC-PC species was examined in this paper. An
443 accurate method using normal-phase HPLC coupled on-line with triple quadrupole mass spectrometer
444 was developed to characterise and quantify all PC species, including VLC-PCs in human retina and
445 bovine retinas. Since the results from molecular and biochemical studies led to the conclusion that
446 VLC-PUFA are involved in the pathogenesis of STD3, the method developed herein may be useful to
447 more accurately investigate the molecular mechanisms leading to photoreceptor dysfunction and
448 death in STD3.

449 **Acknowledgements:**

450 The authors would like to thank Gilles Thuret and Philippe Gain (Faculty of Medicine, Laboratory of
 451 biology, engineering and imaging of corneal graft at Saint Etienne, France) for collecting and providing
 452 retinas from human donors.

453 References

- 454 [1] M.I. Aveladano, J. Biol. Chem. 262 (1987) 1172.
 455 [2] M.I. Aveladano, H. Sprecher, J. Biol. Chem. 262 (1987) 1180..
 456 [3] A. Poulos, Lipids 30 (1995) 1.
 457 [4] N.P. Rotstein, M.I. Aveladano, Biochem. J. 249 (1988) 191.
 458 [5] N.P. Rotstein, M.I. Aveladano, Biochem J. 249 (1988) 191.
 459 [6] Z.Q. Zhang, Y. Wang, H.G. Vikis, L. Johnson, G.J. Liu, J. Li, M.W. Anderson, R.C. Sills, H.L.
 460 Hong, T.R. Devereux, T. Jacks, K.L. Guan, M. You, Na. Genet. 29 (2001) 25.
 461 [7] A.O. Edwards, L.A. Donoso, R. Ritter, Invest. Ophthalmol. Vis. Sci. 42 (2001) 2652.
 462 [8] C. Grayson, R.S. Molday, J. Biol. Chem. 280 (2005) 32521.
 463 [9] P. Tvrdik, R. Westerberg, S. Silve, A. Asadi, A. Jakobsson, B. Cannon, G. Loison, A.
 464 Jacobsson, J. Cell Biol. 149 (2000) 707.
 465 [10] A. Meyer, H. Kirsch, F. Domergue, A. Abbadi, P. Sperling, J. Bauer, P. Cirpus, T.K. Zank, H.
 466 Moreau, T.J. Roscoe, U. Zahringer, E. Heinz, J. Lipid Res. 45 (2004) 1899.
 467 [11] R. Westerberg, P. Tvrdik, A.B. Uden, J.E. Mansson, L. Norlen, A. Jakobsson, W.H. Holleran,
 468 P.M. Elias, A. Asadi, P. Flodby, R. Toftgard, M.R. Capecchi, A. Jacobsson, J. Biol. Chem. 279
 469 (2004) 5621.
 470 [12] J.P. SanGiovanni, E.Y. Chew, Prog. Retin. Eye Res. 24 (2005) 87.
 471 [13] G. Karan, C. Lillo, Z. Yang, D.J. Cameron, K.G. Locke, Y. Zhao, S. Thirumalaichary, C. Li,
 472 D.G. Birch, H.R. Vollmer-Snarr, D.S. Williams, K. Zhang, Proc. Natl. Acad. Sci. U S A 102
 473 (2005) 4164.
 474 [14] A. McMahon, W. Kedzierski, Br. J. Ophthalmol..
 475 [15] M. Agbaga, R.S. Brush, M.N. Mandal, A., K. Henry, M.H. Elliott, R. Anderson, PNAS 105
 476 (2008) 12843.
 477 [16] S.S. Antollini, M.I. Aveladano, J. Lipid Res. 43 (2002) 1440.
 478 [17] J.L. Kerwin, A.R. Tuininga, L.H. Ericsson, J Lipid Res. 35 (1994) 1102.
 479 [18] J. Fang, M.J. Barcelona, J. Microbiol. Methods. 33 (1998) 23.
 480 [19] X. Han, R.W. Gross, J. Am. Soc. Mass Spectro. 6 (1995) 1202.
 481 [20] X. Han, W.G. Richard, Proceedings of the National Academy of Sciences of the United States
 482 of America 91 (1995) 10635.
 483 [21] T. Houjou, K. Yamatani, H. Nakanishi, M. Imagawa, T. Shimizu, R. Taguchi, Rap. Com. Mass
 484 Spectrom. 18 (2004) 3123.
 485 [22] C. Beermann, M. Mobius, N. Winterling, J.J. Schmitt, G. Boehm, lipids 40 (2005) 211.
 486 [23] A. Larsen, S. Uran, P.B. Jacobsen, T. Scotland, Rap. Com. Mass Spectrom. 15 (2001) 2393.
 487 [24] G. Issac, D. Bylund, J.-E. Mansson, K.E. Markides, J. Bergquist, J. Neurosci. Methods. 128
 488 (2003) 111.
 489 [25] A. Carrier, J. Parent, S. Dupuis, J. Chromatogr. A 876 (2000) 97.
 490 [26] B. Barroso, R. Bischoff, J. Chromatogr. B 814 (2005) 21.
 491 [27] E.J. Ahn, H. Kim, B. Chul Chung, G. Kong, M.H. Moon, J. Chromatogr. A 1194 (2008) 90.
 492 [28] E.J. Ahn, H. Kim, B.C. Chung, M.H. Moon, J. Sep. Sci. 30 (2007) 2598.
 493 [29] C.J. Delong, P.R. Baker, M. Samuel, Z. Cui, M.J. Thomas, J. Lipid Res. 42 (2001) 1959.
 494 [30] W.D. Lehmann, M. Koester, E. G., K. Dietrich, Anal. Biochem. 246 (1997) 102.
 495 [31] N. Acar, O. Berdeaux, P. Juaneda, S. Gregoire, S. Cabaret, C. Joffre, C.P. Creuzot-Garcher,
 496 L. Bretilon, A.M. Bron, Exp. Eye Res. (2009) 840.
 497 [32] M. Malavolta, F. Bocci, E. Boselli, N.G. Frega, J. Chromatogr. B 810 (2004) 173.
 498 [33] K.Z. Berry, R.C. Murphy, J. Am. Soc. Mass Spectrom. 15 (2004) 1499.
 499 [34] B. Brugger, G. Erben, R. Sandhoff, F.T. Wielland, W.D. Lehmann, Proceedings of the National
 500 Academy of Sciences of the United States of America 94 (1997) 2339.
 501 [35] F. Gao, X. Tian, W. Dawei, J. Liao, T. Wang, H. Liu, Biochim. Biophys. Acta 1761 (2006) 667.
 502 [36] M. Koivusalo, P. Haimi, L. Heikinheimo, R. Kostainen, P. Somerharju, J. Lipid Res. 42 (2001)
 503 663.
 504 [37] H. Kim, H.K. Min, G. Kong, M.H. Moon, Anal. Bioanal. Chem. 393 (2009) 1649.
 505 [38] H. Kim, E.J. Ahn, M.H. Moon, Analyst 133 (2008) 1656.
 506 [39] X. Han, R.W. Gross, Mass. Spectrom. Rev. 24 (2005) 367.

- 507 [40] M. Pulfer, R.C. Murphy, *Mass. Spectrom. Rev.* 22 (2003) 332.
 508 [41] X. Han, R.W. Gross, *J. Lipid Res.* 44 (2003) 1071.
 509 [42] H. Kim, T.-C. Wang, L., Y.-C. Ma, *Anal. Chem.* 66 (1994) 3977.
 510 [43] M. Hermansson, A. Uphoff, R. Käkälä, P. Somerharju, *Anal. Chem.* 77 (2005) 2166.
 511 [44] R. Taguchi, J. Hayakawa, Y. Takeuchi, M. Ishida, *J. Mass. Spectrom.* 35 (2000) 953.
 512 [45] T. Houjou, K. Yamatani, M. Imagawa, T. Shimizu, R. Taguchi, *Rap. Com. Mass Spectrom.* 19
 513 (2005) 654.
 514 [46] D.N. Heller, R.J. Cotter, C. Fenselau, *Anal. Chem.* 59 (1987) 2806.
 515 [47] L. Bretillon, G. Thuret, S. Gregoire, N. Acar, C. Joffre, A.M. Bron, P. Gain, C.P. Creuzot-
 516 Garcher, *Exp. Eye Res.* 87 (2008) 521.
 517 [48] J. Folch, M. Lees, G.H.S. Standley, *J. Biol. Chem.* 226 (1957) 497.
 518 [49] E.M. Bartlett, D.H. Lewis, *Anal. Biochem.* 36 (1970) 159.
 519 [50] W.R. Morrison, L.M. Smith, *J. Lipid Res.* 5 (1964) 600.
 520 [51] F. Dionisi, P.A. Golay, L.B. Fay, *Anal. Chim. Acta* 465 (2002) 395.
 521 [52] L. Fay, U. Richli, *J. Chromatogr.* 541 (1991) 89.
 522 [53] P. Juaneda, G. Rocquelin, P.O. Astorg, *Lipids* 25 (1990) 756.
 523 [54] W.W. Christie, *J. Lipid Res.* 26 (1985) 507.
 524 [55] M.I. Avelano, *Biochemistry* 27 (1988) 1229.
 525 [56] M. Such, A.A. Wierzbicki, M.T. Clandinin, *Biochim. Biophys. Acta -Lipids and Lipid Metabolism*
 526 1214 (1994) 54.
 527 [57] O. Berdeaux, R. Wolff, *J. Am. Oil Chem. Soc.* 73 (1996) 1323.
 528 [58] J.Y. Zhang, Q.T. Yu, B.N. Liu, Z.H. Huang, *Biomed. Environ. Mass Spectrom.* 15 (1988) 33.
 529 [59] D.J. Cameron, Z.Z. Tong, Z.L. Yang, J. Kaminoh, S. Kamiyah, H.Y. Chen, J.X. Zeng, Y.L.
 530 Chen, L. Luo, K. Zhang, *Int. J. Biol. Sci.* 3 (2007) 111.
 531 [60] V. Vasireddy, Y. Uchida, N. Salem, S.Y. Kim, M.N.A. Mandal, G.B. Reddy, R. Bodepudi, N.L.
 532 Alderson, J.C. Brown, H. Hama, A. Dlugosz, P.M. Elias, W.M. Holleran, R. Ayyagari, *Hum.*
 533 *Mol. Genet.* 16 (2007) 471.
 534 [61] N.E. Furland, E.N. Maldonado, M.I. Avelano, *Lipids* 38 (2003) 73.
 535 [62] M. Rabionet, A.C. van der Spoel, C.C. Chuang, B. von Tumpling-Radosta, M. Litjens, D.
 536 Bouwmeester, C.C. Hellbusch, C. Korner, H. Wiegandt, K. Gorgas, F.M. Platt, H.J. Grone, R.
 537 Sandhoff, *J. Biol. Chem.* 283 (2008) 13357.
 538 [63] V. Vasireddy, M.M. Jablonski, M.N. Mandal, D. Raz-Prag, X.F. Wang, L. Nizol, A. Iannaccone,
 539 D.C. Musch, R.A. Bush, N. Salem, Jr., P.A. Sieving, R. Ayyagari, *Invest. Ophthalmol. Vis. Sci.*
 540 47 (2006) 4558.
 541 [64] D. Raz-Prag, R. Ayyagari, R.N. Fariss, M.N. Mandal, V. Vasireddy, S. Majchrzak, A.L.
 542 Webber, R.A. Bush, N. Salem, Jr., K. Petrukhin, P.A. Sieving, *Invest. Ophthalmol. Vis. Sci.* 47
 543 (2006) 3603.
 544 [65] W. Li, Y. Chen, D.J. Cameron, C. Wang, G. Karan, Z. Yang, Y. Zhao, E. Pearson, H. Chen, C.
 545 Deng, K. Howes, K. Zhang, *Vision Res.* 47 (2007) 714.
 546 [66] F.F. Hsu, A. Bohrer, J. Turk, *J. Am. Soc. Mass Spectrom.* 9 (1997) 516.
 547 [67] C.Y. Lee, A. Lesimple, A. Larsen, O. Mamer, J. Genest, *J. Lipid Res.* 46 (2005) 1213.

548 **Figures legends:**

550 **Figure 1:** (A) LC-ESI-MS normal-phase chromatogram of the lipid extract from bovine retina. The
 551 retention time of phosphatidylethanolamine (PE), phosphatidylinositol (PI), phosphatidylserine (PS),
 552 phosphatidylcholine (PC), sphingomyelin (SM), and lyso-phosphatidylcholine (LPC) classes were 7–
 553 8.5 min, 11–12 min, 12–14 min, 15.5–22 min, and 23–27.5 min, respectively. (B) LC-ESI-MS normal-
 554 phase chromatogram of the lipid extract from human retina. The retention time of PE, PI, PS, PC, SM,
 555 and LPC classes were 7–8 min, 11–12 min, 13–14 min, 15.6–21 min and 23.5–27 min, respectively.
 556 The mass spectrometer was operated under full scan in the negative ion mode from 0 to 15 min and in
 557 the positive ion mode from 15 min to 40 min.

558 **Figure 2:** Product-ion spectra of negative ions of various commercial phosphatidylcholines (PC)
 559 (collision offset, +25 V). (A) Product ion spectrum of the $[M - CH_3]^-$ of PC 16:0/18:1 at m/z 744. (B)
 560 Product ion spectrum of the $[M - CH_3]^-$ of PC 18:0/20:4 at m/z 794. (C) Product ion spectrum of the $[M$

561 $-\text{CH}_3^-$ of PC 18:0/22:6 at m/z 818. (D) Product ion spectrum of the $[\text{M} - \text{CH}_3]^-$ PlsC 18:0/18:1 at m/z
562 756. (E) Product ion spectrum of the $[\text{M} - \text{CH}_3]^-$ PlsC 18:0/22:6 at m/z 802. (F) Product ion spectrum
563 of the $[\text{M} - \text{CH}_3]^-$ of PC 32.4/22:6 at m/z 1006.

564 **Figure 3:** Negative-ion HPLC-ESI-MS analysis of phosphatidylcholine (PC) molecular species from
565 bovine retina. The mass spectrometer was operated under full scan from 650 to 1100 $u\text{m}a$. (A) Mass
566 spectrum of total PC fraction including PC-containing VLC-PUFA (VLC-PC) collected from 15.2 min to
567 22 min, as shown in Figure 1; (B) mass spectrum of VLC-PC fraction from 15.2 min to 16.8 min, as
568 shown in Figure 1.

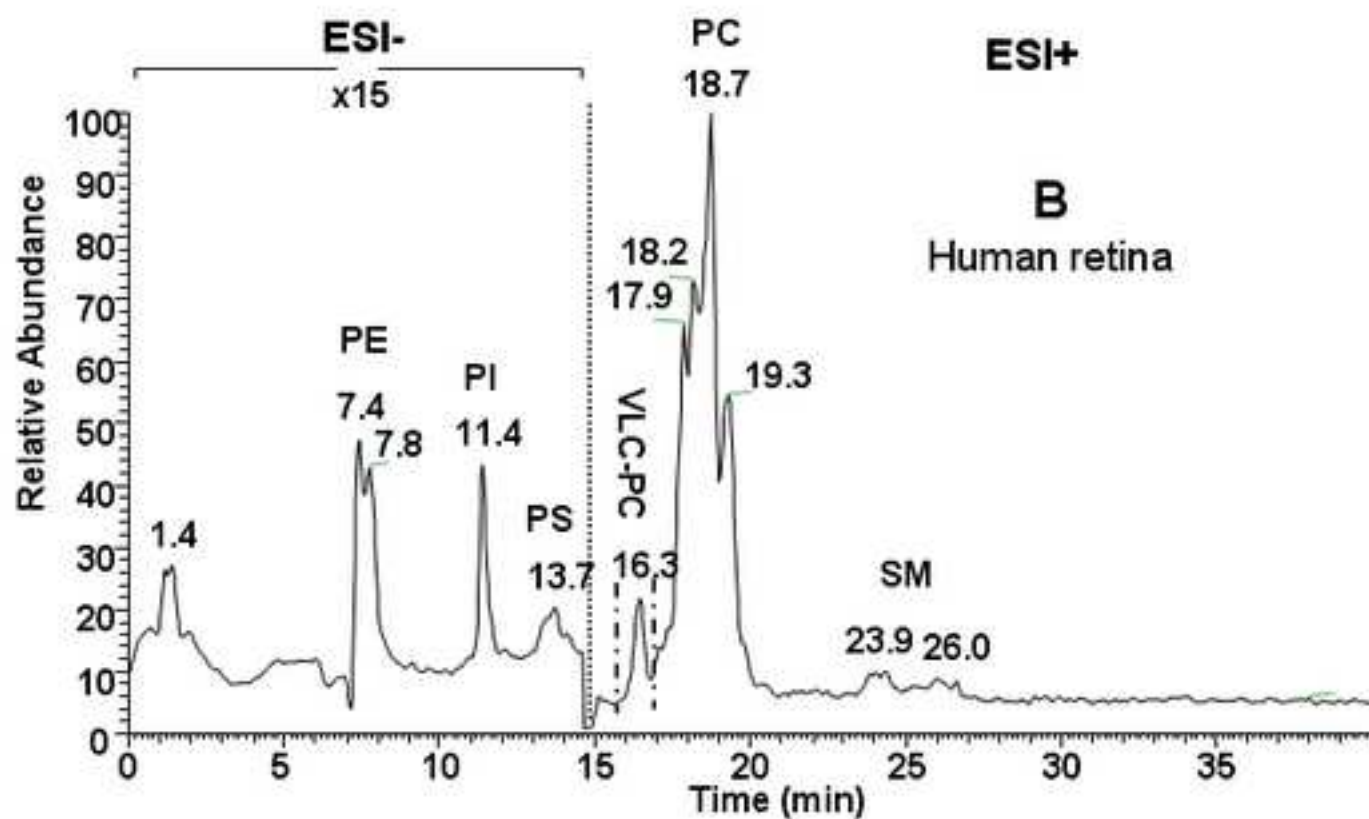
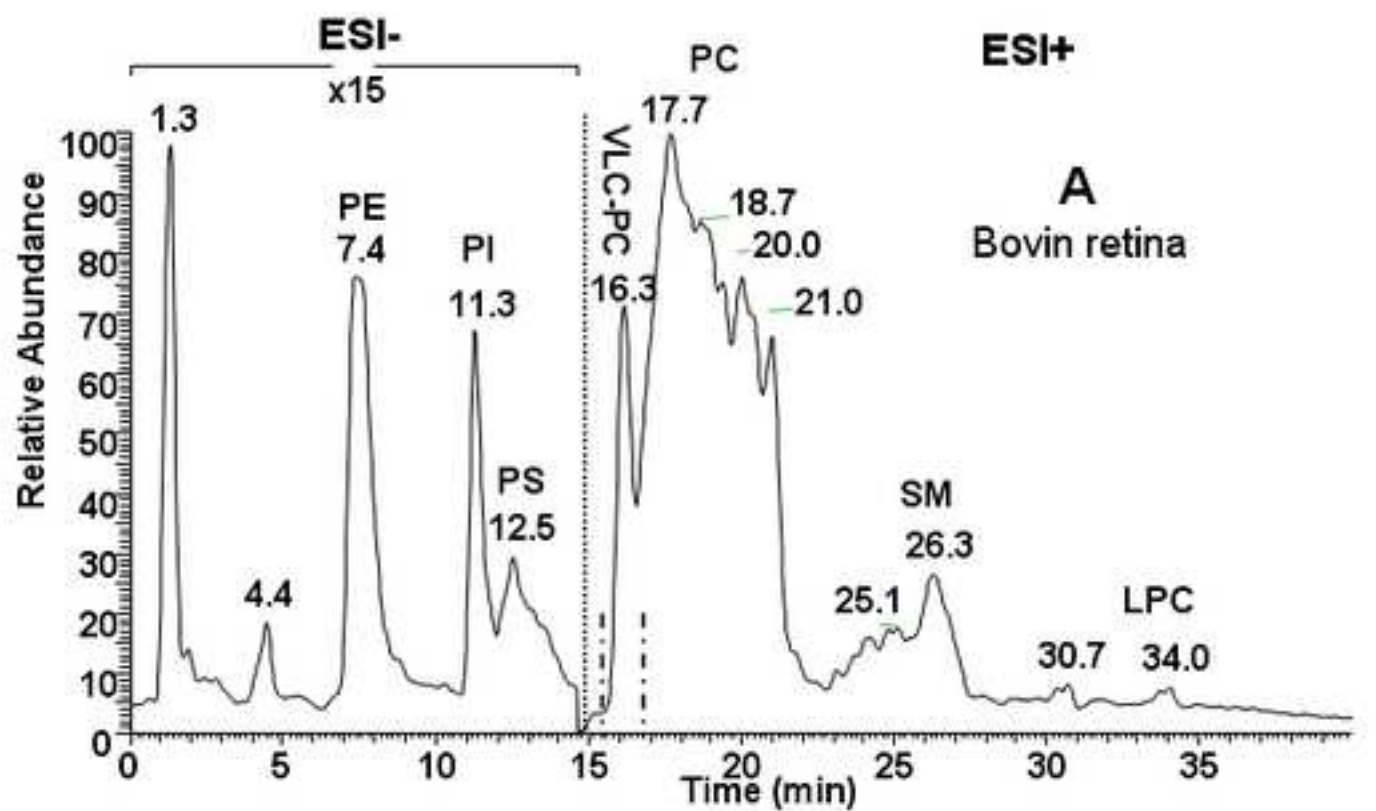
569 **Figure 4:** Negative-ion HPLC-ESI-MS mass spectrum of total phosphatidylcholine (PC) fraction
570 including PC-containing VLC-PUFA (VLC-PC) collected from 15.6 min to 21 min, as shown in Figure
571 6. The mass spectrometer was operated under full scan from 650 to 1100 $u\text{m}a$.

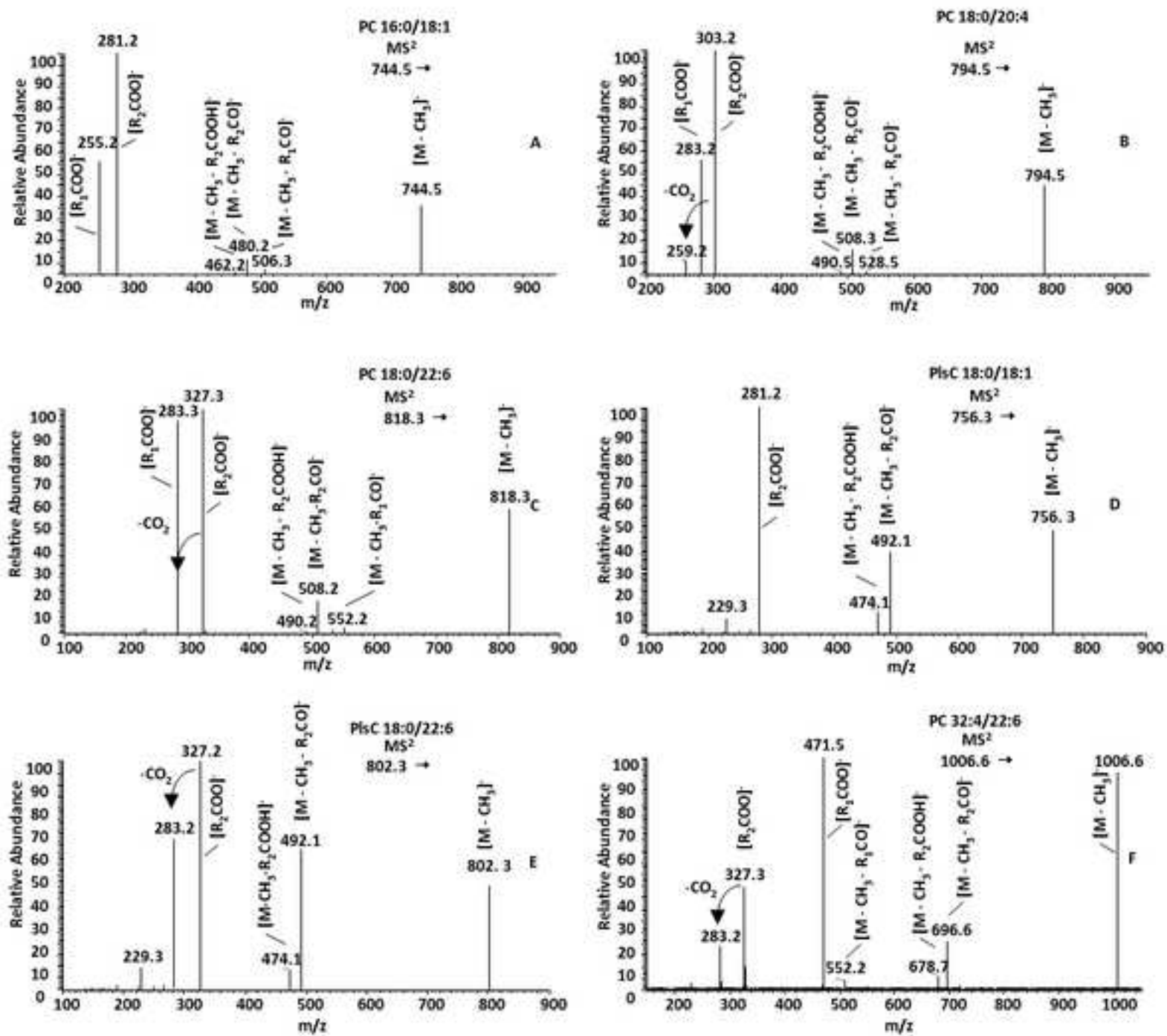
572 **Figure 5:** Partial GC-EI-MS total ion chromatograms (BPX-70 column) of (A) 4,4-dimethyloxazoline
573 (DMOX) derivatives of the isolated VLC-PC fraction obtained from bovine retina and (B) DMOX
574 derivatives of the isolated VLC-PC fraction obtained from human retina.

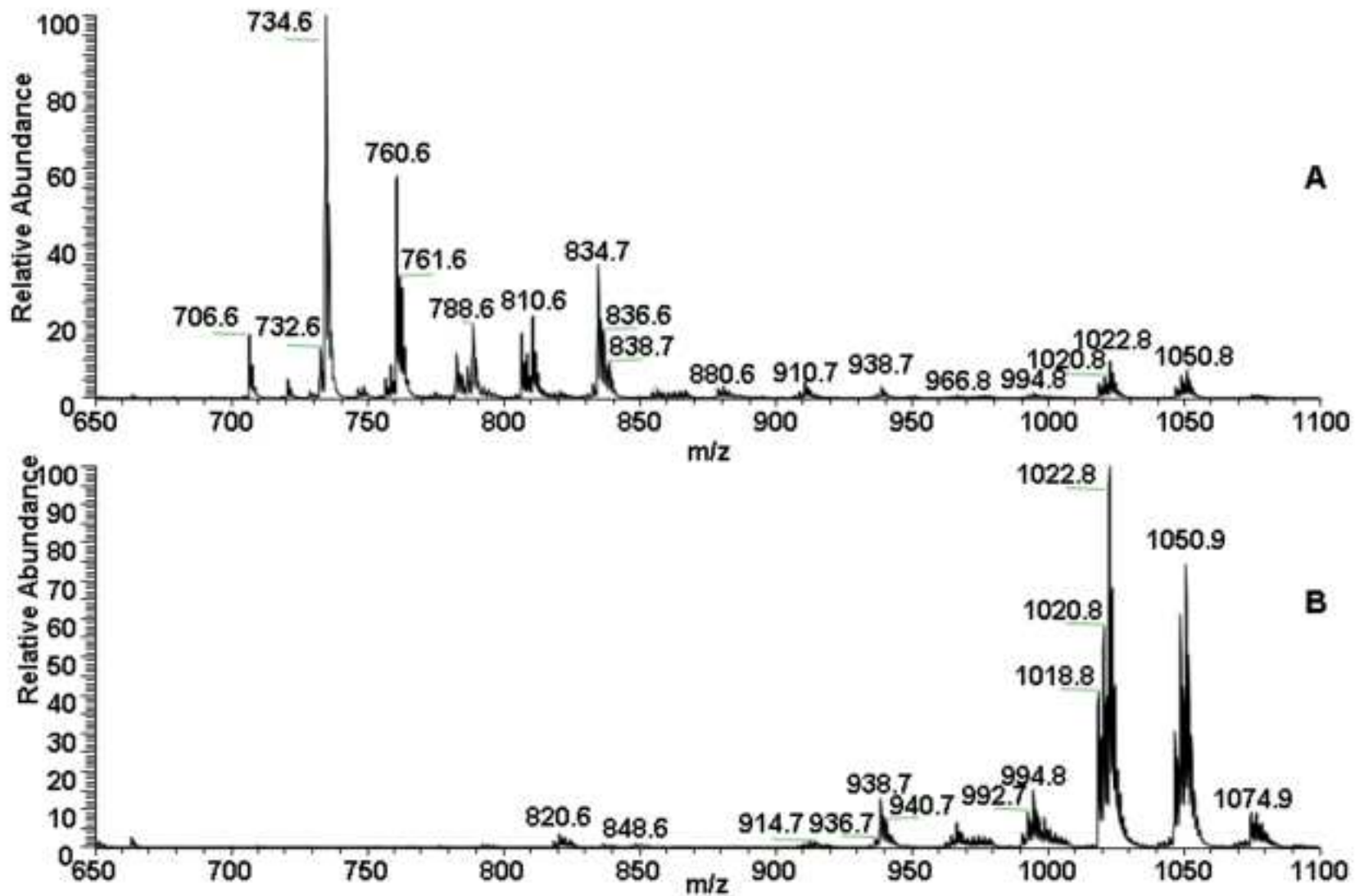
575 **Figure 6:** Mass spectra of 4,4-dimethyloxazoline (DMOX) derivatives of (A) 32:4n-6 and (B) 32:6n-3.

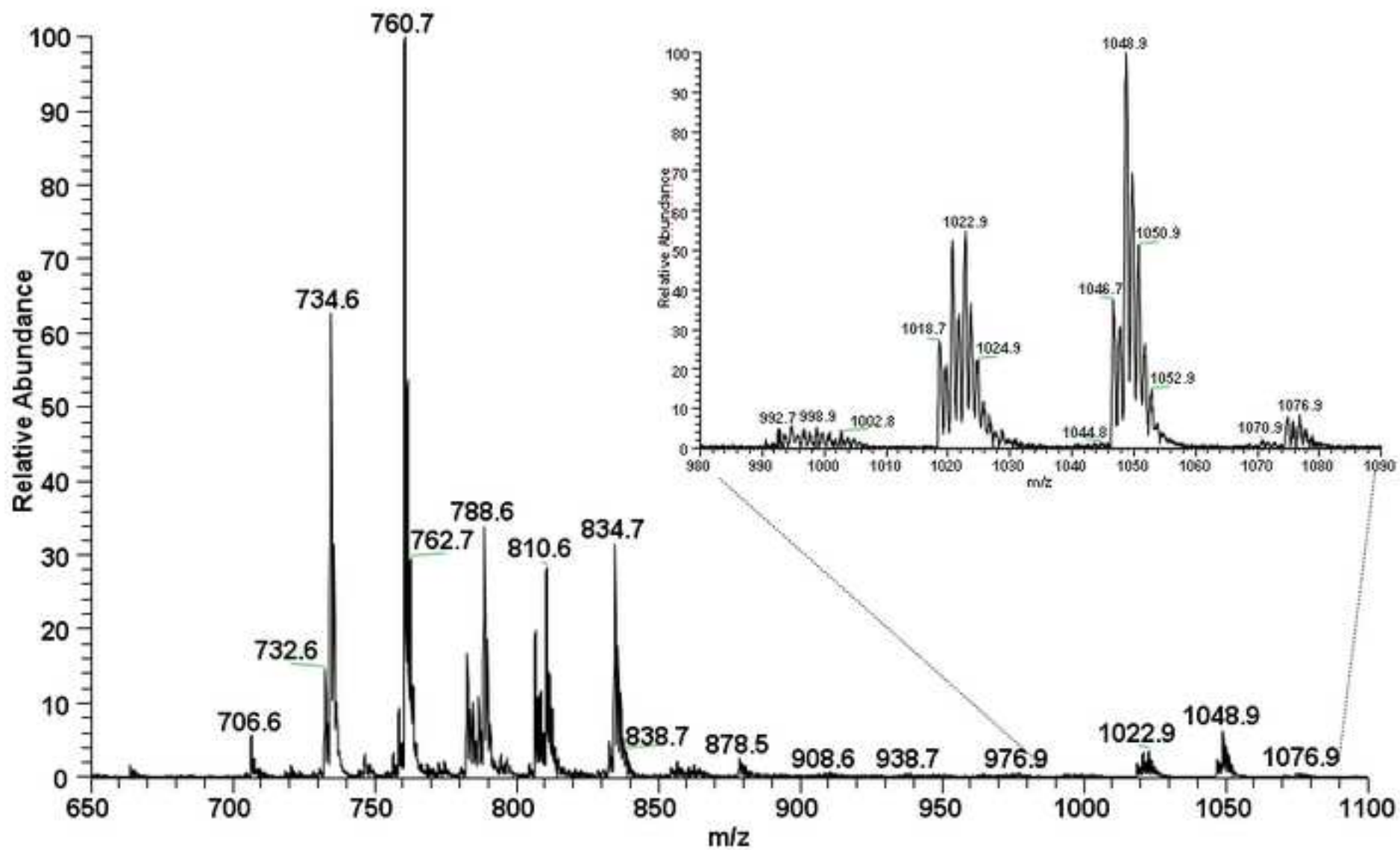
576 **Figure 7:** Concentration dependency of instrument responses. An equimolar mixture of 12 saturated
577 phosphatidylcholine (PC) species was prepared, diluted from 5 $\text{pg}/\mu\text{L}$ to 5 $\text{ng}/\mu\text{L}$ per species (from 60
578 $\text{pg}/\mu\text{L}$ to 60 $\text{ng}/\mu\text{L}$ of total PC) in chloroform/methanol (1:1) and then analyses using HPLC-ESI-MS by
579 scanning for precursors of m/z 184 in the positive mode. Total peak intensity versus concentration of
580 total PC.

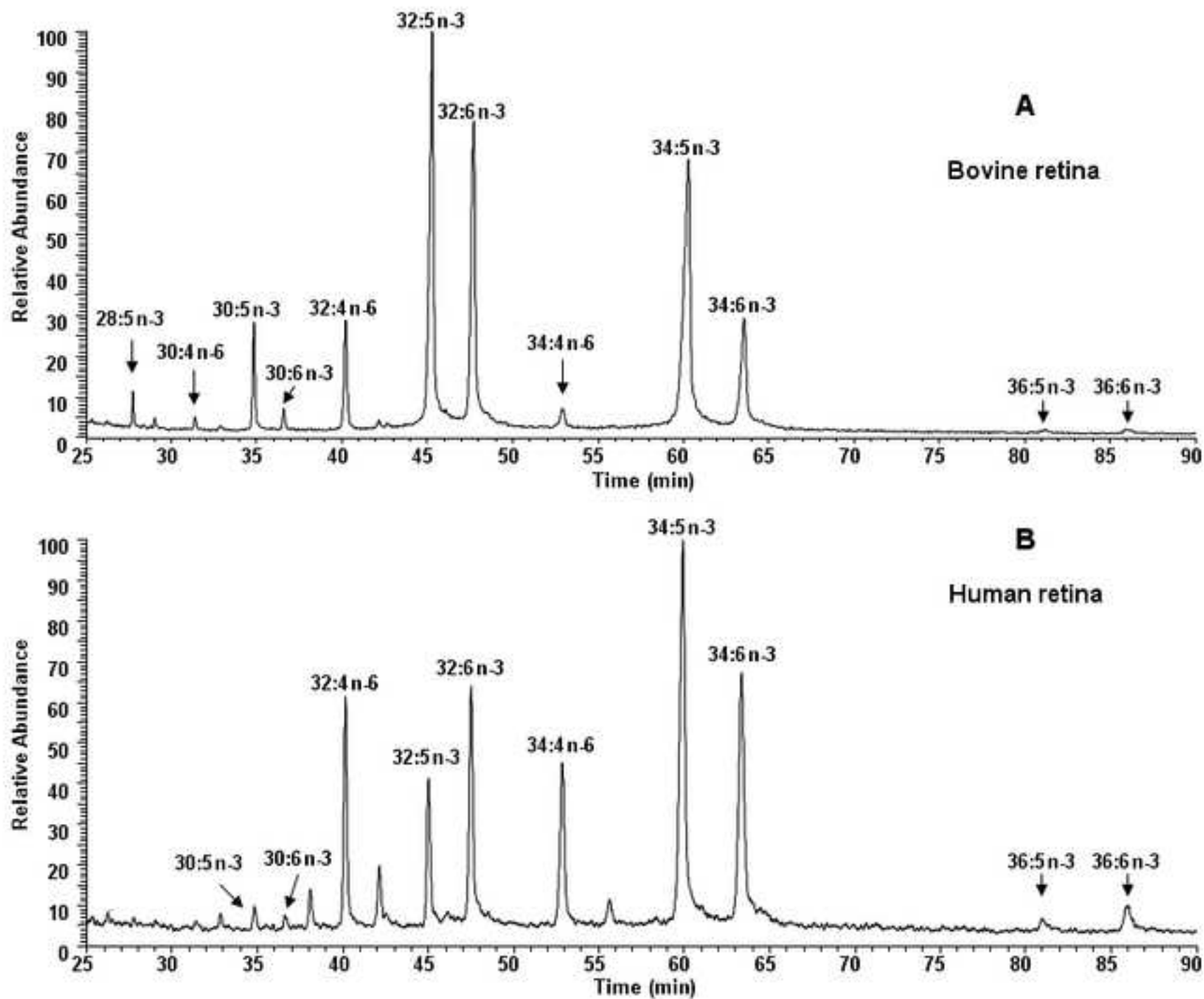
581 **Figure 8:** Positive-ion HPLC-ESI-MS analysis of an equimolar mixture of four phosphatidylcholine
582 (PC) standards (1 $\text{ng}/\mu\text{L}$ each) spiked in total lipid extract from human retina (12.5 $\text{ng}/\mu\text{L}$) by parent ion
583 scanning at -36 V collision offset. The dashed lines indicate the dependency of instrument response
584 on m/z . The main indicated PC species are m/z 678.4 = PC 28:0 (std); m/z 706.6 = PC 30:0, m/z 734
585 = PC 32:0, m/z 760 = PC 34:1, m/z 790.4 = PC 36:0 (std); m/z 834 = PC 40:6, m/z 846 = PC 44:0
586 (std); m/z 930 = PC 46:0 (std), m/z 958 = PC 48:0 (std); m/z 1022 = PC 54:10 and m/z 1050 = PC
587 56:10.

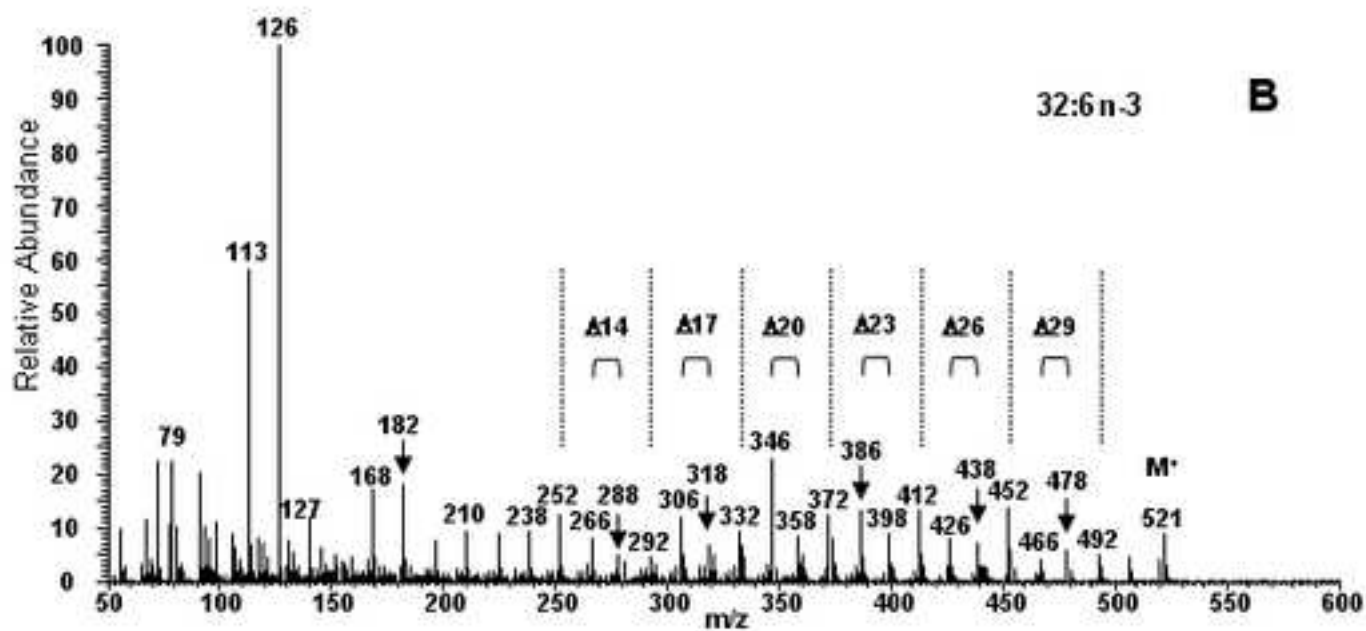
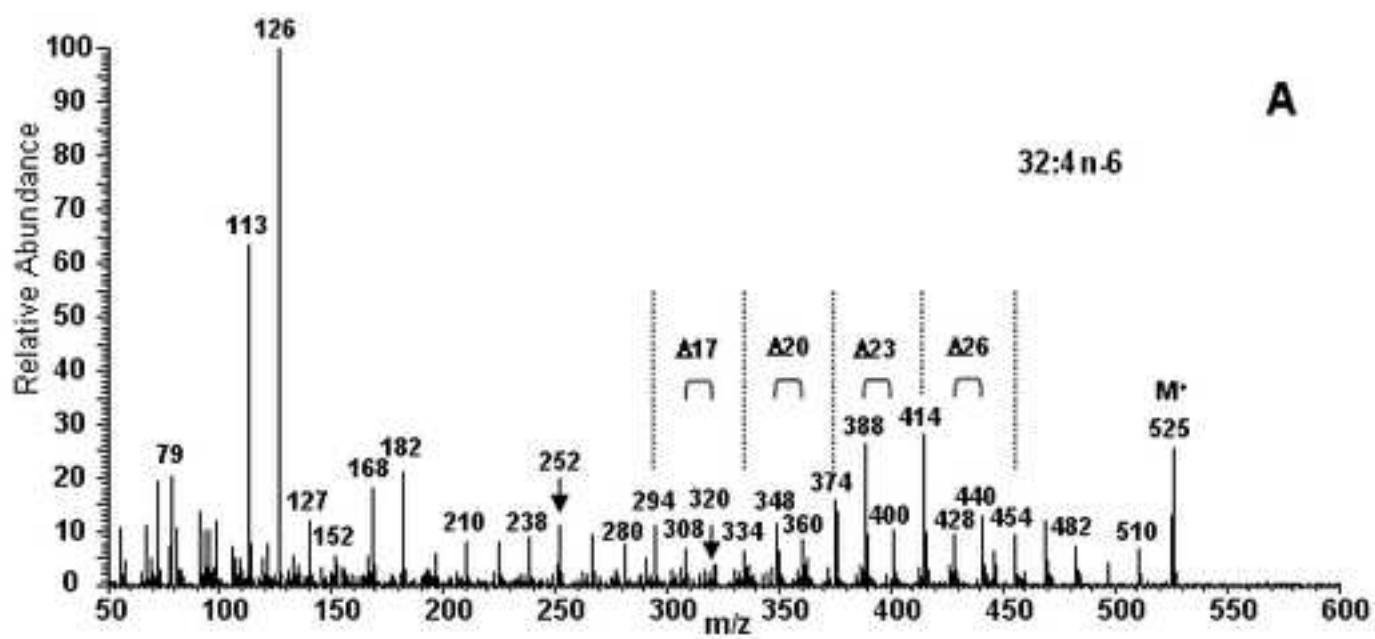


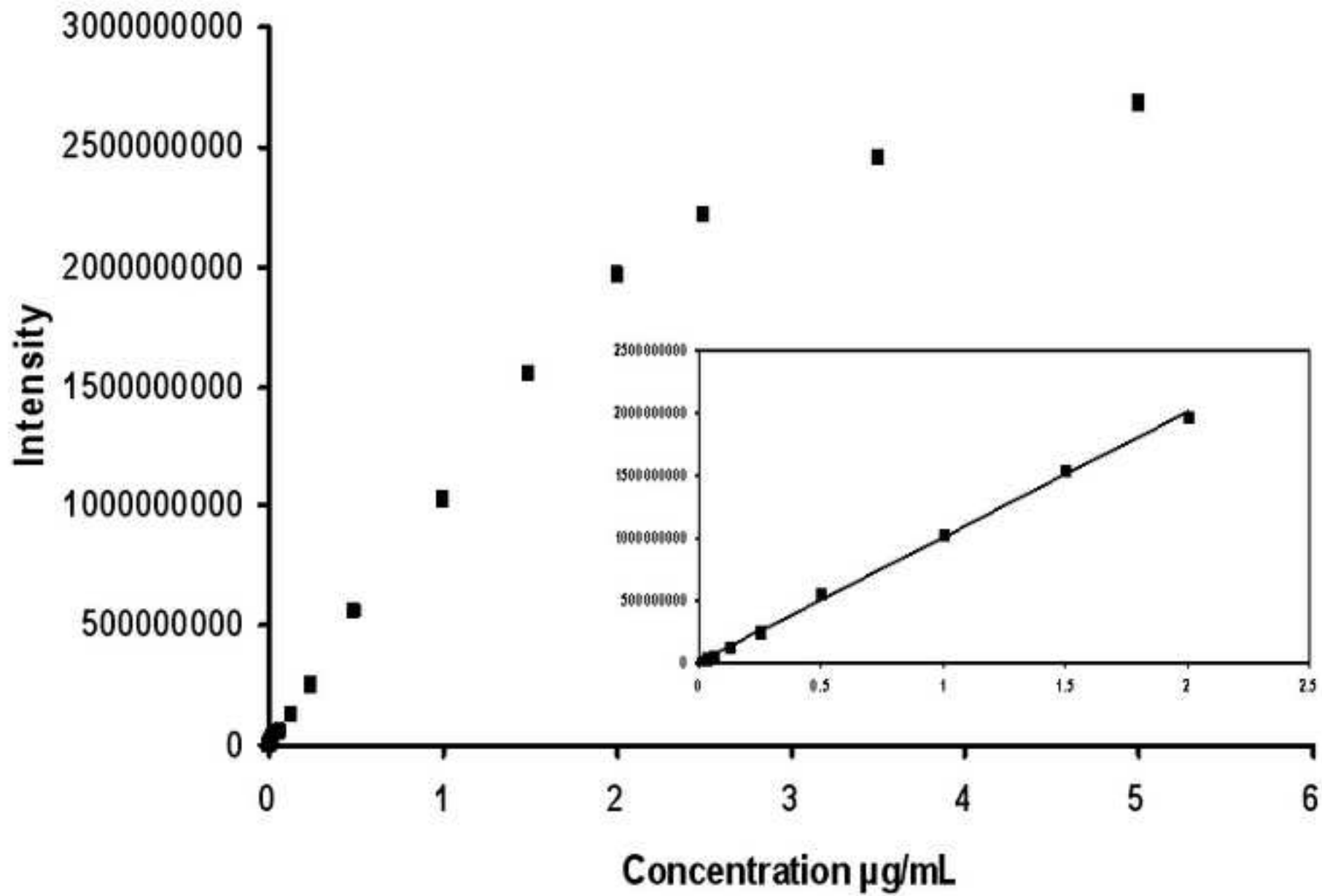












Manuscript

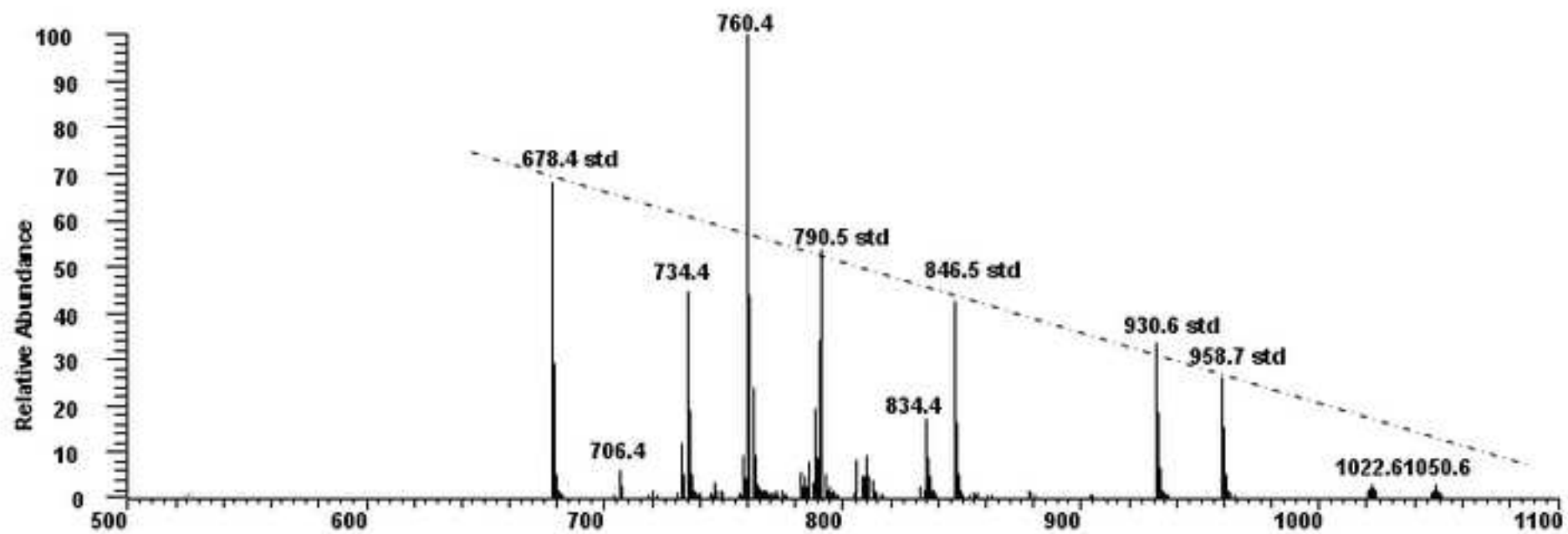


Table 1: Characterization of phosphatidylcholine molecular species in total lipid extract from bovine retina.

Molecular species		ESI-			ESI+	Retention time (min)	
		[M-CH ₃]	[R ₁ CH ₂ COO]	[R ₂ CH ₂ COO]	[M+H] ⁺		
PC 30:0	PC 14:0/16:0	690.4		227.4	255.4	706.4	20.9
PlsC 32:1	PlsC p160/16:1	704.6			253.4	720.6	20.7
PC 32:2	PC 16:1/16:1	714.5		253.4	253.4	730.5	20.6
PC 32:1	PC 16:0/16:1	716.5		255.4	253.4	732.5	20.5
PC 32:0	PC 16:0/16:0*	718.5		255.4	255.4	734.6	20.0
PlsC 34:0	PlsC p180/16:0	730.5			253.4	746.5	17.2
PC 34:2	PC 16:0/18:2	742.6		255.4	279.4	758.6	18.9
PC 34:1	PC 16:0/18:1*	744.6		255.4	281.4	760.6	18.7
PC 34:0	PC 16:0/18:0	746.6		255.4	283.4	762.6	19.0
PlsC 36:0	PlsC p180/18:0	758.6			281.5	774.6	17.2
PC 36:4	PC 16:0/20:4	766.6		255.4	303.5	782.6	17.0
PC 36:3	PC 18:1/18:2	768.6		281.5	279.4	784.6	18.4
PC 36:2	PC 18:1/18:1	770.6		281.5	281.5	786.6	18.3
PC 36:2	PC 18:0/18:2	770.6		283.5	279.4	786.6	18.3
PC 36:1	PC 18:0/18:1	772.3		283.5	281.5	788.3	18.3
PC 36:0	PC 18:0/18:0*	774.7		283.4	283.5	790.7	18.3
PlsC 38:6	PlsC p160/22:6	774.7			327.5	790.7	17.2
PlsC 38:5	PlsC p181/20:4	776.7			303.5	792.7	17.1
	PlsC p160/22:5	776.7			329.5	792.7	17.1
PlsC 38:4	PlsC p180/20:4	778.7			303.5	794.7	17.0
	PlsC p160/22:4	778.7			331.5	794.7	17.0
PlsC 38:3	PlsC p180/20:3	780.7			305.5	796.7	16.9
	PlsC p18:1/20:2	780.7			308.5	796.7	16.9
PC 38:6	PC 18:2/20:4	790.5		279.4	303.5	806.6	18.0
	PC 16:0/22:6	790.5		255.4	327.5	806.6	18.0
PC 38:5	PC 18:1/20:4	792.5		281.5	303.5	808.6	17.9
	PC 16:0/22:5	792.5		255.4	329.5	808.6	17.9
PC 38:4	PC 18:0/20:4*	794.6		283.5	303.5	810.6	17.5
PC 38:3	PC 18:0/20:3	796.6		283.5	305.5	812.6	17.8
PlsC 40:6	PlsC p180/22:6*	802.6			327.5	818.6	16.9
PlsC 40:5	PlsC p181/22:4	804.6			331.5	820.6	16.8
	PlsC p180/22:5	804.6			329.5	820.6	16.6
PlsC 40:4	PlsC p180/22:4	806.6			331.5	822.7	16.6
PlsC 40:3	PlsC p181/22:2	808.6			335.5	824.7	16.5
PlsC 40:2	PlsC p181/22:1	810.5			337.6	826.6	16.5
PC 40:7	PC 18:1/22:6	816.6		281.5	327.5	832.6	17.6
PC 40:6	PC 18:0/22:6*	818.6		283.5	327.5	834.7	17.6
PC 40:5	PC 18:0/22:5	820.6		283.5	329.5	836.6	17.3
	PC 18:1/22:4	820.6		281.5	331.5	836.6	17.3
PC 40:4	PC 18:0/22:4	822.6		283.5	331.5	838.6	17.3
PC 44:12	PC 22.6/22:6	862.6		327.5	327.5	878.6	17.1
PC 44:11	PC 22.5/22:6	864.6		329.5	327.5	880.6	17.0
PC 44:10	PC 22.4/22:6	866.6		331.5	327.5	882.6	17.2
PC 44:9	PC 22:3/22:6	868.6		333.5	327.5	884.6	17.2
PC 46:12	PC 24:6/22:6	890.6		355.6	327.5	906.6	17.0
PC 46:11	PC 24.5/22:6	892.7		357.6	327.5	908.7	17.0
PC 46:10	PC 24.4/22:6	894.7		359.6	327.5	910.7	16.9
PC 46:9	PC 24:3/22:6	896.7		361.6	327.5	912.7	16.9
PC 48:12	PC 26:6/22:6*	918.7		383.7	327.5	934.7	16.9
PC 48:11	PC 26:5/22:6	920.7		385.7	327.5	936.7	16.8
PC 48:10	PC 26:4/22:6	922.7		387.5	327.5	938.7	16.8
PC 50:12	PC 28:6/22:6	946.7		411.7	327.5	962.7	16.8
PC 50:11	PC 28:5/22:6	948.7		413.7	327.5	964.7	16.6
PC 50:10	PC 28.4/22:6	950.0		415.7	327.5	966.0	16.5
PC 52:12	PC 30:6/22:6	974.7		439.7	327.5	990.7	16.5
PC 52:11	PC 30:5/22:6	976.8		441.7	327.5	992.8	16.5
PC 52:10	PC 30:4/22:6	978.8		443.7	327.5	994.8	16.4
PC 54:12	PC 32:6/22:6	1 002.7		467.7	327.5	1 018.8	16.5
PC 54:11	PC 32:5/22:6	1 004.7		469.8	327.5	1 020.8	16.3
PC 54:10	PC 32:4/22:6	1 006.8		471.8	327.5	1 022.8	16.3
PC 56:12	PC 34:6/22:6	1 030.8		495.8	327.5	1 046.8	16.2
PC 56:11	PC 34:5/22:6	1 032.8		497.8	327.5	1 048.8	16.2
PC 56:10	PC 34:4/22:6	1 034.8		499.8	327.5	1 050.8	16.1
PC 58:12	PC 36:6/22:6	1 058.8		523.9	327.5	1 074.8	16.0
PC 58:11	PC 36:5/22:6	1 060.8		525.9	327.5	1 076.9	15.9
PC 58:10	PC 36.4/22:6	1 062.8		527.9	327.5	1 078.9	15.9

* Commercial standards availables and used for identification and the calibration curves

Table 2: Characterization and quantification of phosphatidylcholine molecular species in total lipid extract from human neural retina from 9 donors.

Molecular species		Characterization				Quantification								
		ESI-			ESI+	($\mu\text{g/mL}$)								
		[M-CH ₃] ⁻	[R ₁ CH ₂ COO] ⁻	[R ₂ CH ₂ COO] ⁻	[M+H] ⁺	1	2	3	4	5	6	7	8	9
PC 14:0/16:0	PC 30:0	690.4	227.4	255.4	706.4	0.089	0.113	0.072	0.092	0.095	0.084	0.083	0.108	0.069
PlsC p160/16:1	PlsC 32:1	704.0		253.4	720.0	0.016	0.033	0.025	0.027	0.029	0.023	0.026	0.032	0.021
PC 16:1/16:1	PC 32:2	714.5	253.4	253.4	730.5	0.029	0.021	0.013	0.022	0.016	0.016	0.022	0.018	0.019
PC 16:0/16:1	PC 32:1	716.5	255.4	253.4	732.5	0.274	0.266	0.191	0.232	0.178	0.187	0.219	0.222	0.222
PC 16:0/16:0	PC 32:0	718.6	255.4	255.4	734.6	0.723	0.812	0.642	0.769	0.785	0.822	0.765	0.855	0.669
PlsC p160/18:0	PlsC 34:0	730.6		253.4	746.6	0.065	0.093	0.059	0.061	0.053	0.056	0.049	0.076	0.050
PC 16:0/18:2	PC 34:2	742.6	255.4	279.4	758.6	0.201	0.226	0.188	0.175	0.155	0.162	0.016	0.178	0.166
PC 16:0/18:1	PC 34:1	744.6	255.4	281.4	760.6	1.938	2.188	2.016	1.839	1.912	1.999	1.858	2.006	2.101
PC 16:0/18:0	PC 34:0	746.6	255.4	283.4	762.6	0.288	0.348	0.267	0.298	0.316	0.333	0.276	0.312	0.272
PC 16:0/20:4	PC 36:4	766.6	255.4	303.5	782.6	0.127	0.127	0.133	0.184	0.153	0.160	0.158	0.121	0.164
PC 18:1/18:2	PC 36:3	768.6	281.5	279.4	784.6	0.088	0.090	0.069	0.106	0.090	0.094	0.105	0.093	0.084
PC 18:1/18:1	PC 36:2	770.6	281.5	281.5	786.6	0.153	0.190	0.142	0.113	0.126	0.131	0.107	0.166	0.138
PC 18:0/18:1	PC 36:1	772.6	283.5	281.5	788.6	0.441	0.557	0.371	0.440	0.465	0.489	0.398	0.425	0.432
PC 18:2/20:4	PC 38:6	790.6	279.4	303.5	806.6	0.180	0.153	0.168	0.169	0.182	0.199	0.220	0.192	0.147
PC 18:1/20:4	PC 38:5	792.6	281.5	303.5	808.6	0.126	0.095	0.084	0.099	0.086	0.096	0.087	0.095	0.090
PC 18:0/20:4	PC 38:4	794.6	283.5	303.5	810.6	0.270	0.286	0.229	0.371	0.253	0.297	0.291	0.243	0.300
PC 18:0/20:3	PC 38:3	796.6	283.5	305.5	812.6	0.078	0.076	0.051	0.085	0.077	0.063	0.092	0.074	0.082
PlsC p181/22:6	PlsC 40:7	800.4		327.5	816.4	0.007	0.007	0.007	tr	0.007	0.006	0.003	0.004	0.007
PlsC p181/22:4	PlsC 40:5	804.6		331.5	820.6	0.011	0.009	0.006	0.010	0.007	0.008	0.008	0.008	0.008
PC 18:1/22:6	PC 40:7	816.6	281.5	327.5	832.6	0.056	0.043	0.044	0.043	0.051	0.052	0.045	0.053	0.044
PC 18:0/22:6	PC 40:6	818.6	283.5	327.5	834.6	0.467	0.314	0.327	0.456	0.397	0.425	0.532	0.425	0.404
PC 18:0/22:5	PC 40:5	820.6	283.5	329.5	836.6	0.092	0.059	0.060	0.112	0.088	0.085	0.107	0.077	0.083
PC 22:6/22:6	PC 44:12	862.6	327.5	327.5	878.6	0.048	0.015	0.013	0.008	0.011	0.025	0.017	0.044	0.013
PC 24:6/22:6	PC 46:12	890.6	355.6	327.5	906.6	tr	tr	tr	tr	tr	tr	tr	tr	tr
PC 24:5/22:6	PC 46:11	892.6	357.6	327.5	908.6	tr	tr	tr	tr	tr	0.005	tr	tr	tr
PC 24:4/22:6	PC 46:10	894.6	359.6	327.5	910.6	tr	tr	tr	tr	tr	tr	tr	tr	tr
PC 30:6/22:6	PC 52:12	974.7	439.7	327.5	990.7	tr	tr	tr	tr	tr	tr	tr	tr	tr
PC 30:5/22:6	PC 52:11	976.7	441.7	327.5	992.7	tr	tr	tr	tr	tr	tr	tr	tr	tr
PC 32:6/22:6	PC 54:12	1002.8	467.7	327.5	1018.8	0.022	0.009	0.006	0.020	0.019	0.031	0.021	0.014	0.007
PC 32:5/22:6	PC 54:11	1004.8	469.8	327.5	1020.8	0.022	0.009	0.006	0.020	0.019	0.031	0.021	0.014	0.007
PC 32:4/22:6	PC 54:10	1006.8	471.8	327.5	1022.8	0.023	0.005	0.005	0.036	0.023	0.010	0.020	0.015	0.012
PC 34:6/22:6	PC 56:12	1030.8	495.8	327.5	1046.8	0.030	0.010	0.018	0.024	0.024	0.016	0.038	0.028	0.023
PC 34:5/22:6	PC 56:11	1032.8	497.8	327.5	1048.8	0.065	0.028	0.035	0.055	0.053	0.053	0.071	0.049	0.039
PC 34:4/22:6	PC 56:10	1034.8	499.8	327.5	1050.8	tr	tr	tr	tr	tr	tr	tr	tr	tr
PC 36:6/22:6	PC 58:12	1058.8	523.9	327.5	1074.8	0.015	0.005	0.012	0.009	0.011	0.005	0.010	0.009	0.020
PC 36:5/22:6	PC 58:11	1060.9	525.9	327.5	1076.9	0.011	tr	0.007	0.008	tr	tr	0.007	0.004	0.011

tr < 0.005